

AD _____
(Leave blank)

Award Number: W81XWH-07-1-0064

TITLE: The Role of Lymphangiogenesis in Orthotopic Prostatic Tumor-Environment on
Regional and Systemic Metastasis

PRINCIPAL INVESTIGATOR: Jeremy Bryant Burton

CONTRACTING ORGANIZATION: University of California
Los, Angeles, CA 90095

REPORT DATE: January 2008

TYPE OF REPORT: Annual Summary

PREPARED FOR: U.S. Army Medical Research and Materiel Command
Fort Detrick, Maryland 21702-5012

DISTRIBUTION STATEMENT: (Check one)

☒ X Approved for public release; distribution unlimited

☐ Distribution limited to U.S. Government agencies only;
report contains proprietary information

The views, opinions and/or findings contained in this report are those of the author(s) and should not be construed as an official Department of the Army position, policy or decision unless so designated by other documentation.

REPORT DOCUMENTATION PAGE				Form Approved OMB No. 0704-0188	
Public reporting burden for this collection of information is estimated to average 1 hour per response, including the time for reviewing instructions, searching existing data sources, gathering and maintaining the data needed, and completing and reviewing this collection of information. Send comments regarding this burden estimate or any other aspect of this collection of information, including suggestions for reducing this burden to Department of Defense, Washington Headquarters Services, Directorate for Information Operations and Reports (0704-0188), 1215 Jefferson Davis Highway, Suite 1204, Arlington, VA 22202-4302. Respondents should be aware that notwithstanding any other provision of law, no person shall be subject to any penalty for failing to comply with a collection of information if it does not display a currently valid OMB control number. PLEASE DO NOT RETURN YOUR FORM TO THE ABOVE ADDRESS.					
1. REPORT DATE 31-01-2008		2. REPORT TYPE Annual Summary		3. DATES COVERED 1 JAN 2007 - 31 DEC 2007	
4. TITLE AND SUBTITLE The Role of Lymphangiogenesis in Orthotopic Prostatic Tumor-Environment on Regional and Systemic Metastasis				5a. CONTRACT NUMBER	
				5b. GRANT NUMBER W81XWH-07-1-0064	
				5c. PROGRAM ELEMENT NUMBER	
6. AUTHOR(S) Jeremy Bryant Burton Email: jbburton@ucla.edu				5d. PROJECT NUMBER	
				5e. TASK NUMBER	
				5f. WORK UNIT NUMBER	
7. PERFORMING ORGANIZATION NAME(S) AND ADDRESS(ES) University of California Los Angeles, CA 90095				8. PERFORMING ORGANIZATION REPORT NUMBER	
9. SPONSORING / MONITORING AGENCY NAME(S) AND ADDRESS(ES) U.S. Army Medical Research and Materiel Command Fort Detrick, Maryland 21702-5012				10. SPONSOR/MONITOR'S ACRONYM(S)	
				11. SPONSOR/MONITOR'S REPORT NUMBER(S)	
12. DISTRIBUTION / AVAILABILITY STATEMENT Approved for Public Release; Distribution Unlimited					
13. SUPPLEMENTARY NOTES					
14. ABSTRACT The extent of tumor-associated lymphangiogenesis augments lymphatic metastasis in many tumors types, although there have been limited studies in prostate cancer. Interestingly, we found that the metastatic potential of several prostate cancer xenografts is directly correlated with the expression of lymphangiogenic factor, VEGF-C. We utilized soluble VEGFR-3 and therapeutic antibody (a-mVEGFR-3, mF4-31C1, ImClone Inc.) to block VEGF-C/VEGFR-3 signaling in the more aggressive CWR22Rv-1 tumor. The expression of soluble VEGFR-3 in CWR22Rv-1 resulted in a significant reduction in intratumoral lymphatic vasculature, as well as metastasis to both regional lymph node and lung. These results indicate that tumor lymphangiogenesis is a key factor contributing to local regional lymph nodes and systemic metastasis in prostate cancer models. Hence, inhibiting tumor lymphangiogenesis may be a promising therapeutic strategy to suppress the deadly consequence of systemic metastasis of prostate cancer.					
15. SUBJECT TERMS Lymphangiogenesis, Angiogenesis, Prostate Cancer, VEGF-C, Xenograft, Orthotopic					
16. SECURITY CLASSIFICATION OF:			17. LIMITATION OF ABSTRACT	18. NUMBER OF PAGES	19a. NAME OF RESPONSIBLE PERSON
a. REPORT	b. ABSTRACT	c. THIS PAGE			USAMRMC
U	U	U	UU	60	19b. TELEPHONE NUMBER (include area code)

Table of Contents

	<u>Page</u>
Introduction.....	4
Body.....	5-12
Supplemental Figures.....	13-14
Key Research Accomplishments.....	15
Reportable Outcomes.....	16
Conclusion.....	17
References.....	17
Appendices.....	18-60
Manuscript.....	18-57
Curriculum Vitae.....	58-60

Introduction

Pelvic lymph node metastasis in prostate cancer is associated with poor patient prognosis and clinical outcome(1). The extent of tumor-associated lymphangiogenesis augments lymphatic metastasis in many tumors types, although there have been limited studies in prostate cancer. Interestingly, we found that the metastatic potential of several prostate cancer xenografts is directly correlated with the expression of pro-lymphangiogenic factor, VEGF-C(2). To examine the contribution of tumor lymphangiogenesis to metastasis, we over-expressed lymphangiogenic growth factors in the non-metastatic LAPC-9 model expressing luciferase. An increase in intratumoral lymphangiogenesis, but not angiogenesis, enhanced both lymph node and lung metastasis. In converse experiments of down-regulation of lymphangiogenesis, we utilized soluble VEGFR-3 and therapeutic antibody (α -mVEGFR-3, mF4-31C1, ImClone Inc.) to block VEGF-C/VEGFR-3 signaling in the more aggressive CWR22Rv-1 tumor. The expression of soluble VEGFR-3 in CWR22Rv-1 resulted in a significant reduction in intratumoral lymphatic vasculature, as well as metastasis to both regional lymph node and lung. These results indicate that tumor lymphangiogenesis is a key factor contributing to local regional lymph nodes and systemic metastasis in prostate cancer models. Hence, inhibiting tumor lymphangiogenesis may be a promising therapeutic strategy to suppress the deadly consequence of systemic metastasis of prostate cancer.

Specific Aims (restated)

Aim #1 To investigate the influence of lymphangiogenesis on metastasis in an orthotopically implanted xenograft model

Aim #2 To investigate the feasibility of preventing metastasis by inhibiting lymphangiogenesis during metastatic progression of murine prostate cancer model Pten (-/-).

Research Accomplishments

Task 1 (restated). To assess the influence of lymphangiogenesis in orthotopic implantation of LAPC-9 xenograft (Month 1-11):

- a) Complete the generation of PSE-BC/VEGF-C lentiviral vector and grow up virus (month 1-2).
- b) Transduce tumor cells with lentiviral vectors and perform assays to assure modulated expression of VEGF-C (month 3-4).
- c) Implant and monitor tumor growth and metastasis in 8 mice/group; 1) CMV/empty vector (control), CMV/VEGF-C, PSE-BC/VEGF-C, and CMV/sVEGFR3 (4-8 months).
- d) Perform histology on all collected tissues and tumors (month 8-11)

Rationale of task 1 (restated)

LAPC-9 metastasizes readily from the subcutis upon induction of lymphangiogenesis. Our preliminary results suggest that lymphatics in the margin of the tumor are sufficient to disseminate tumor cells regionally and systemically. LAPC-9 represents an ideal

model to test the influence of the pre-existing lymphatics in the prostate in tumor metastasis because 1) LAPC-9 has already been shown to metastasize in the presence of increased lymphatic vasculature in subcutaneously implanted tumors, and 2) LAPC-9 expresses very low levels of lymphangiogenic growth factor VEGF-C. We propose that modulation of VEGF-C expression and signaling in LAPC-9 will allow us to determine the role of lymphangiogenesis in metastasis. In order to achieve modulated VEGF-C expression, strong (CMV) and moderate (PSA enhanced, PSE-BC) promoters will be utilized to drive expression compared to wild-type LAPC-9, which will function as a "low expression" model. In addition, we will also over-express sVEGFR-3 to inhibit lymphangiogenesis. This strategy will allow us to compare high (CMV), moderate (PSE-BC), low (wt LAPC-9), and suppressed (sVEGFR-3) levels of VEGF-C in a model that readily metastasizes in the presence of lymphatics. Using optical imaging we will monitor metastasis and quantify luminescence in regional lymph nodes and organs.

Update on task 1a.

The intraprostatic implanted LAPC-9/VEGF-C/GFP/RL tumors display an extensive network of peritumoral lymphatics extending into the margin of the tumor (**Figure 1**). Interestingly, even without forced VEGF-C expression, the orthotopic implanted LAPC-9 prostate tumors displayed extensive peritumoral lymphatics (**figure 2a**). Furthermore, when LAPC-9 tumors were implanted in the blood and lymphatic vasculature rich environment of the mouse prostate gland, we detected a propensity for nodal metastasis even in the absence of added lymphangiogenic drive (**Figure 2b,c**). Therefore, rather than modulating VEGF-C expression using high and low activity

promoters (CMV and PSEBC, respectively), we proceeded by inhibiting lymphangiogenesis in LAPC-9 using soluble VEGFR-3 receptor expression and VEGF-C RNA interference.

Update on task 1b-d.

To understand the role of lymphatics in the metastasis of prostate cancer, we evaluated the influence of vascular endothelial growth factor by 1) soluble VEGFR-3 receptor inhibition in a orthotopic model of LAPC-9, and 2) over-expression of lentivirus mediated shRNA against VEGF-C in this same model. Our results suggest a critical role of VEGF-C in mediating lymphangiogenesis and metastatic spread, which is dependent on the prostatic microenvironment.

- **Soluble VEGFR-3 receptor inhibition in an orthotopic model of LAPC-9.**

Please see attached manuscript (Cancer Res) for a complete description of the effects of sVEGFR-3 on LAPC-9 metastasis. This manuscript was accepted to the journal Cancer Research for publication in October, 2008. Overall these data indicates that LAPC-9, although weakly lymphangiogenic subcutaneously, noticeably induces lymphangiogenesis orthotopically, which leads to lymph node metastasis. This process is VEGFR-3 dependent since soluble VEGFR-3 expression reduces this lymphangiogenesis and metastasis.

- **Lentivirus mediated shRNA against VEGF-C in LAPC-9**

We proceeded to determine the precise role of tumor VEGF-C expression in orthotopic lymphangiogenesis and regional lymph node metastasis. We transduced LAPC-9 tumors cells with a lentiviral vector expressing a short-hairpin RNA targeting human VEGF-C under control of polIII promoter, U6. LAPC-9 cells

expressing Renilla luciferase and VEGF-C shRNA or irrelevant firefly luciferase shRNA (Ctrl) were implanted orthotopically as before. To determine the level by which VEGF-C expression was reduced, tumors were removed at endpoint, RNA was extracted, and real-time RTPCR was performed using primers specific to VEGF-C and Actin for internal control. VEGF-C expression was reduced to by 81% in the shVEGF-C group compared to ctrl (**figure 4a**). Analysis of the optical signal in periaortic (**figure 4b**) and mesenteric (**figure 4c**) lymph nodes revealed a 80% and 90% reduction in tumor cell dissemination in shVEGF-C cohort relative to ctrl.

Once again we examined the impact on tumor lymphangiogenesis by examining the interface between the normal prostate region and the tumor. Control LAPC-9 tumors retained the extensive marginal lymphatics as observed in **figure 3**. By contrast, the shVEGF-C tumors had reduced vasculature that was discontinuous and punctate, without vessel extension into the tumor margin (**figure 4d**). We next examined the VEGF-C expression level in LAPC-9 implanted subcutaneously and orthotopically to determine if the prostatic environment stimulates had a higher VEGF-C level or stimulated a higher level in the tumor, by some unknown stromal factor. Comparing VEGF-C expression using primers specific for mouse (stroma) or human (tumor) VEGF-C, we found essential no expression of VEGF-C outside of that provided by the tumor cells (**figure 4e**). In addition, there is no difference in the expression of VEGF-C grown subcutaneously or orthotopically (**figure 4f**). Ultimately, the finding suggest that the greater density of pre-existing lymphatics creates an environment in which reduced lymphangiogenic growth factor expression is sufficient to stimulate lymphangiogenesis. Alternatively, the lymphatics in the

prostate may be primed for VEGF-C induced lymphangiogenesis by the expression of alternative growth factors.

Current status of task 1

Task 1 is complete

Task 2 (restated). To evaluate the influence of sVEGFR-3 overexpression on metastasis in Pten knockout model (Month 10-24):

- a) Generate Ubc/sVEGFR-3 and Ubc/Renilla luciferase (RL) lentiviral vectors by subcloning gene directly from CMV/sVEGFR-3 or CMV/RL (month 10).
- b) Characterize VEGF-C expression in Pten(-/-) mice using prostatic tissues from each stage of progression (month 10-12)
- c) Monitor efficiency of Ubc/lentiviral transduction and expression in Pten (-/-) prostate using optical imaging of Renilla luciferase (month 10-16).
- d) Characterized influence of lentiviral mediated sVEGFR-3 expression on Pten (-/-) metastatic progression compared to empty vector control; 16 mice/group (month 14-19).
- e) Perform histology on all collected tissues and tumors (month 18-24)

Rationale of task 2 (restated).

Metastasis is a multi-step process that depends on accumulated cellular alteration in order to acquire a state of dedifferentiation that allows for anchorage independent survival and invasiveness into surrounding vasculature networks, both of which are required for metastasis. Prostate cancer is a progressive disease that proceeds through a

series of histologically defined steps including prostatic hyperplasia, intraepithelial neoplasia, and invasive adenocarcinoma(3). The *Pten* knockout model recapitulates many of the clinical features of this progression. Additionally, our preliminary results suggest that *Pten* progression to invasive adenocarcinoma is marked by an increase in lymphatic number and lumen size, hallmarks of lymphangiogenesis(4). This model thereby provides a unique opportunity to investigate the influence of VEGF-C signaling on prostate tumor progression and metastasis. In doing so we can begin to understand the interplay between acquired metastatic states of tumor cells and the process of invasiveness into vasculature. We hypothesize that inhibition of VEGF-C signaling during *Pten* progression will reduce the incidents of lymph node and possibly systemic metastasis.

Update on Task 2a,c.

Replacing the existing CMV promoter in lenti-vector pCCL-RL with the PGK promoter from vector pRRL-shluc-PGK-GFP generated a lentiviral vector expressing Renilla luciferase under control of PGK promoter. PGK was utilized instead of ubiquitin because of the availability of PGK in our lab and several previous studies have utilized PGK as a promoter for constitutive expression in transgenic animal. Lentivirus, termed pCCL-PGK-RL was generated and concentrated by ultracentrifugation at 25,000 x gravity for 1 hour.

Due to difficulty with obtaining *Pten* knockout mice in numbers sufficient for the study detailed in task 2d, we utilized the Tramp model instead. This model is generated by prostate restricted overexpression of the SV40 T-antigen, which leads to defined stages in the progression to prostate cancer similar to those described for *Pten*(5). The

prostate of a Tramp mouse was surgically exposed and injected with 20 μ l ($\sim 5 \times 10^6$ particles) of lentivirus pCCL-PGK-RL into the dorsolateral prostate. After one month the mice prostates were removed and optically imaged for Renilla luciferase expression. The overall signal intensity was considerably lower than expected, so much so that the signal could only be observed ex vivo. Given the enormous amounts of virus that would be required to successfully undertake task 2d, I decided to pursue alternatives to suppression of lymphangiogenesis in Tramp model. To that end, we obtained a therapeutic monoclonal antibody against mouse VEGFR-3 (mF4-31C1, α -R3) from Imclone Systems Inc. In addition we obtained a VEGFR-2 antibody called DC101 to investigate the impact of angiogenesis on metastasis. While the mF4-31C1 has been shown to inhibit VEGFR-3 dependent tumor lymphangiogenesis in other models, it has not been shown for prostate cancer xenografts. Therefore, we proceeded to determine if it would be effective in inhibiting prostate xenograft CWR22Rv-1 lymphangiogenesis and metastasis.

- **Effects of antibody-mediated VEGFR-2 and VEGFR-3 blockade on tumor growth and metastasis in orthotopic CWR22Rv-1 tumors.**

Please see attached manuscript (Appendix) for a complete description of the effects of therapeutic antibody on CWR22Rv-1 lymphangiogenesis and metastasis. This manuscript was accepted to the journal Cancer Research for publication in October, 2008. Overall these data indicates that the α R-3 therapy is highly effective in inhibiting lymphangiogenesis and metastasis in this xenograft model. Given the effectiveness of the antibody therapy in this model, I will pursue the use of VEGFR-3 antibody therapy in TRAMP mice to examine progression, as stated in task 2d-e.

Update task 2d,e

The TRAMP model effectively recapitulates the clinical characteristics of prostate cancer progression, from preneoplastic lesions to frank carcinoma and metastatic disease(5). Periaortic lymph node metastasis can be found in 20% of TRAMP mice at 24 weeks of age, although as the disease progressed beyond this time period mice frequently developed systemic metastasis(5). Since the majority of mice develop prostatic intraepithelial neoplasia (PIN) lesions by 16 weeks of age, I will initiate antibody therapy at this time. Mice will receive 800µg/mouse mF4-31C1 or PBS, every other day until 24 weeks, at which time mice will be sacrificed. Lymph nodes and lungs will be harvested and examined by histology for metastasis. In addition the primary tumors will be sectioned and stained for lymphatic vessels to examine the impact of VEGFR-3 blockade in modulating lymphangiogenesis.

Current status of task 2.

TRAMP mice are being treated and will be sacrificed this September 2008. Tissues will be processed according to task 2e.

Supplemental Figures

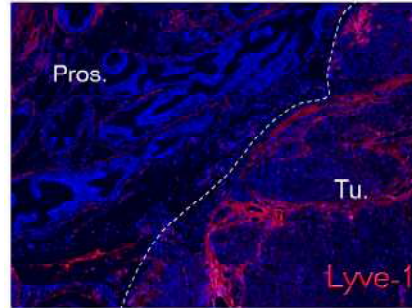


Figure 1. Lymphatic vessels (Lyve-1, red) penetrate the tumor margin at the interface with the mouse prostate (Pros.) to invade the LAPC-9 tumor (Tu.)

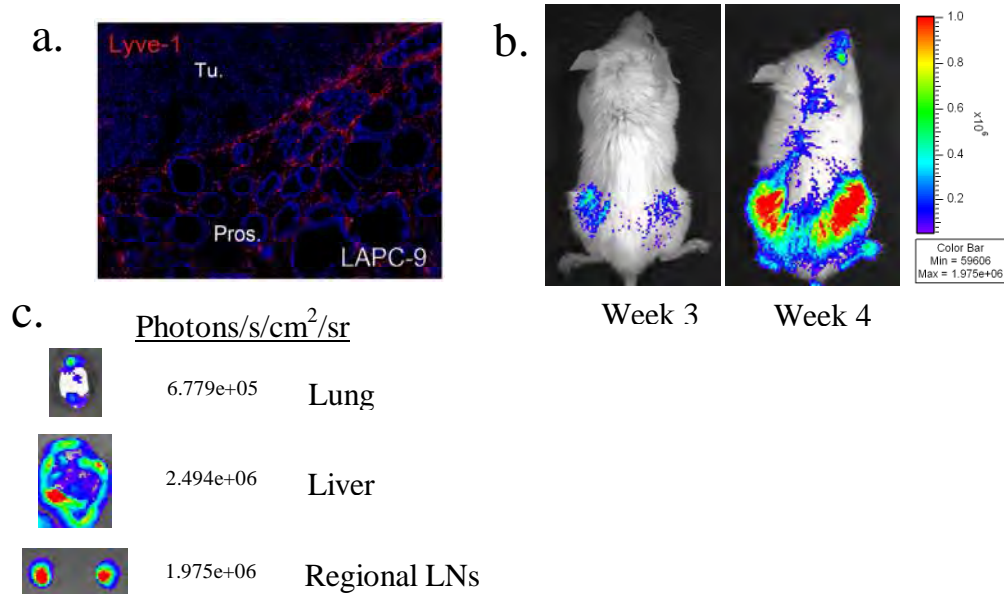


Figure 2. Lymphatics of orthotopically implanted xenografts. **a)** Small punctuate lymphatic vessels can be observed throughout the prostatic region associated with the LAPC-9 tumor. LAPC-9/RL tumors were implanted into the dorsolateral prostates of Scid/Beige mice. **b)** Mice were imaged after 3 and 4 weeks, revealing spreading of tumor cells. **c)** Organs were extracted at 4 week time point and imaged ex vivo for renilla luciferase expressing tumor cells. Metastasis was observed in lung, liver, and lymph nodes.

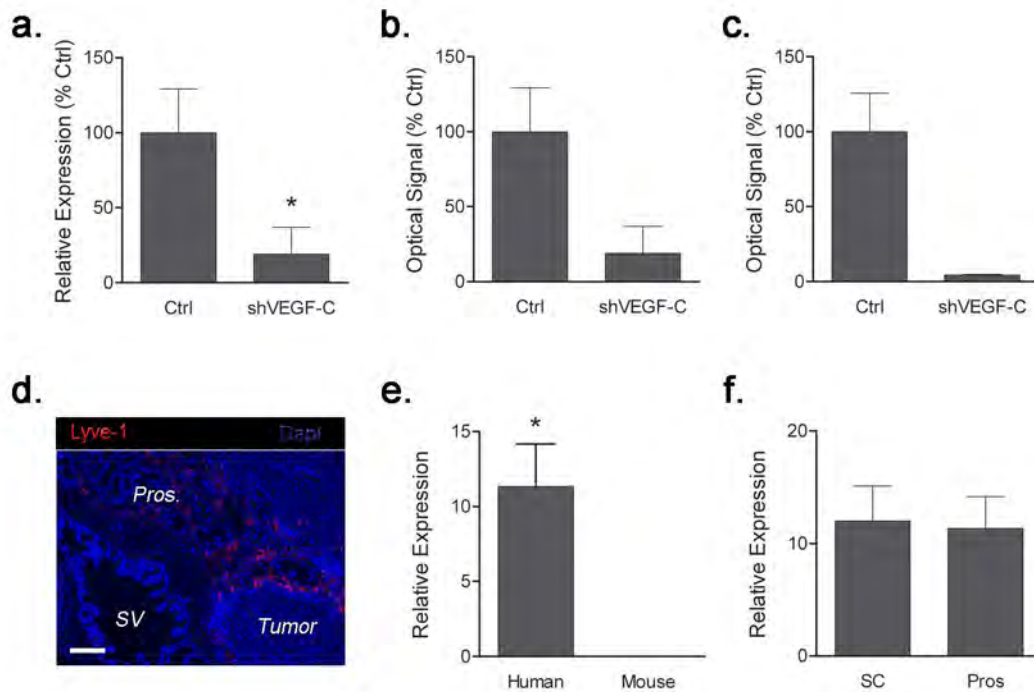


Figure 3: VEGF-C RNA interference inhibits regional lymph node metastasis in orthotopic LAPC-9. (a) VEGF-C expression was measured by real time RTPCR in tumors expressing irrelevant fluc shRNA or VEGF-C shRNA. VEGF-C shRNA reduced expression to 19% of the Ctrl. Lymph node signal was reduced by 80% in periaortic (b) and >90% in mesenteric (c) lymph nodes. (d) Tumors were again sectioned and stained for Lyve-1 positive vessels. Positive staining regions are sporadic and punctate, similar to those tumors expressing sVEGFR-3. (e) Using primers specific for human or mouse VEGF-C, real time PCR was unable to detect VEGF-C in the surrounding tumor stroma. (f) Also no difference in human VEGF-C expression was observed between ctrl tumors grown subcutaneously (sc) or orthotopically (pros). Scale bars is 20μm, (d) Pros=prostate; SV=seminal vesicle.

Key Research Accomplishments

- Employing several methods to modulate vascular signaling, I revealed distinct roles for VEGF and VEGF-C in promoting tumor angiogenesis, lymphangiogenesis, and metastasis in prostate xenograft models
- Showed that anti-lymphangiogenic therapies, not only reduced metastasis to regional pelvic lymph nodes but also to vital organs such as lung.
- Showed that sensitive bioluminescent imaging technique facilitates the tracking and quantification of metastases.
- Found that orthotopic environment greatly influences lymphangiogenic potential by reducing the threshold for VEGFR-3/VEGF-C paracrine signaling.
- Demonstrated the therapeutic potential of VEGFR-3 antibody for reducing lymph node metastasis in an aggressive prostate xenograft model, CWR22Rv-1.

Reportable Outcomes

- Awarded Doctor of Philosophy (PhD) Degree in Medical and Molecular Pharmacology; June 2008. University of California, Los Angeles. PI: Dr. Lily Wu

Manuscripts:

- Brakenhielm, E.*, **Burton, J.B.***, Johnson, M., Chavarria, N., Morizono, K., Chen, I., Alitalo, K., Wu, L. (2007) Modulating metastasis by a lymphangiogenic switch in prostate cancer. *Int. J. Cancer*. **121** (10) p. 2153-61.
- **Burton, J.B.**, Johnson, M., Sato, M., Koh, S., Stout, D., Chatziioannou, A.F., Phelps, M., Wu, L. (2008). Adenovirus Mediated Gene Expression Imaging to Directly Detect Sentinel Lymph Node Metastasis of Prostate Cancer. *Nat. Med.* **14** (8) p. 882-8.
- **Burton, J.B.**, Priceman, S.J., Sung, J.L., Pytowski, B., Alitalo, K., Wu, L. (2008). Suppression of Prostate Cancer Nodal and Systemic Metastasis by Blockade of the Lymphangiogenic Axis. In Press *Cancer Res.* October 2008.

(*, co-first author)

Conclusion

Tumor lymphatic vessels play a crucial role in metastasis in our xenograft models. Using molecular techniques to parse the vascular pathways we found that VEGFR-3 dependent lymphangiogenesis contributes to this metastatic spread. While pre-existing lymphatics in the prostate can mediate spread of tumor cells to periaortic lymph nodes, tumor-mediated lymphangiogenesis greatly contributes to the spread by generating vascular beds at the prostate/tumor interface. Our initial strategy to drive the VEGF-C/VEGFR-3 axis by forced over-expression of vascular growth factors revealed interesting information related to the importance of invasive lymphatics in dissemination to lymph nodes, as well as the influence of lymphatic metastasis on systemic spread. Showing that similar results could be obtained through suppressing the VEGF-C/VEGFR-3 axis in the more aggressive model, CWR22RV-1, with soluble receptor traps and therapeutic antibodies served to strengthen these findings.

References

1. S. Daneshmand *et al.*, *J Urol* **172**, 2252-5 (Dec, 2004).
2. E. Brakenhielm *et al.*, *Int J Cancer* **121**, 2153-61 (Nov 15, 2007).
3. K. P. Porkka, T. Visakorpi, *Eur Urol* **45**, 683-91 (Jun, 2004).
4. M. G. Achen, B. K. McColl, S. A. Stacker, *Cancer Cell* **7**, 121-7 (Feb, 2005).
5. J. R. Gingrich, R. J. Barrios, B. A. Foster, N. M. Greenberg, *Prostate Cancer Prostatic Dis* **2**, 70-75 (Mar, 1999).

Suppression of Prostate Cancer Nodal and Systemic Metastasis by Blockade of the Lymphangiogenic Axis

Jeremy B. Burton^{1*}, Saul J. Priceman^{1*}, James L. Sung¹, Ebba Brakenhielm^{2, 6}, Dong Sung An³, Bronislaw Pytowski⁴, Kari Alitalo⁵, Lily Wu^{1,2‡}

¹Department Molecular and Medical Pharmacology, ²Department of Urology, ³AIDS Institute, Crump Institute for Molecular Imaging, and Jonsson Comprehensive Cancer Center, David Geffen School of Medicine, University of California Los Angeles

⁴Department of Cell Biology, ImClone Systems, New York.

⁵Molecular/Cancer Biology Laboratory and Ludwig Institute for Cancer Research, Biomedicum Helsinki, Haartman Institute and Helsinki University Central Hospital, University of Helsinki, Helsinki, Finland

⁶Rouen Medico-Pharmacological University, Rouen, France

Words in abstract:	210			
Words in paper:	5315	(excluding	references,	figure legends,
acknowledgements)				
Pages:	37			
Figures:	5, 1 supplemental			
References:	44			

Running title: Inhibiting Prostate Cancer Nodal Metastasis

Key words: Lymph Node, Lymphangiogenesis, Angiogenesis, Prostate, Metastasis, Luciferase

* Authors contributed equally

Abstract

Lymph node involvement denotes a poor outcome for patients with prostate cancer. Our group, along with others, has shown that initial tumor cell dissemination to regional lymph nodes via lymphatics also promotes systemic metastasis in mouse models. The aim of this study was to investigate the efficacy of suppressive therapies targeting either the angiogenic or lymphangiogenic axis in inhibiting regional lymph node and systemic metastasis in subcutaneous and orthotopic prostate tumor xenografts. Both androgen-dependent and more aggressive, androgen-independent prostate tumors were employed in our investigations. Interestingly, we observed that the threshold for dissemination is lower in the vascular-rich prostatic microenvironment compared to subcutaneously grafted tumors. Both VEGF-C ligand trap (sVEGFR-3) and antibody directed against VEGFR-3 (mF4-31C1) significantly reduced tumor lymphangiogenesis and metastasis to regional lymph node and distal vital organs, without influencing tumor growth. Conversely, angiogenic blockade by short-hairpin RNA against VEGF or anti-VEGFR-2 antibody (DC101) reduced tumor blood vessel density, significantly delayed tumor growth, and reduced systemic metastasis, although was ineffective in reducing lymphangiogenesis or nodal metastasis. Collectively, these data clarify the utility of vascular therapeutics in prostate tumor growth and metastasis, particularly in the context of the prostate microenvironment. Our findings highlight the importance of lymphangiogenic therapies in the control of regional lymph node and systemic metastasis.

Introduction

Prostate cancer is the most common cancer among men and is second in cancer-related deaths in the United States (1). While monitoring serum PSA and histopathology (Gleason grade) are useful in clinical assessment, pelvic lymph node metastasis remains the most significant indicator of patient prognosis and determinant of therapeutic aggressiveness (2, 3). As prostate carcinoma progresses, systemic metastasis to bone and liver ultimately lead to patient morbidity and mortality. Current treatments include radical prostatectomy, usually with pelvic lymphadenectomy for lymph node assessment, followed by radiation or hormone therapy (4). There are currently no effective treatments for recurrent or metastatic disease, highlighting the importance of alternative strategies for early intervention.

Angiogenesis is essential for the growth of solid cancers beyond two millimeters, which is the limit of nutrient diffusion (5). This process also clearly contributes to metastasis of most solid cancers. Vascular Endothelial Growth Factor-A (VEGF) signaling through its receptor VEGFR-2 is critical for the development and maintenance of tumor blood vasculature (6, 7). Inhibition of VEGF signaling, by targeting either the ligand or the receptor, suppresses both tumor growth and metastasis and is currently being tested in clinical trials as single agents and in combination with chemotherapy or radiation therapy (6, 8, 9). More recently, lymphangiogenesis has received much attention as an important mediator of tumor cell dissemination. VEGF-C and VEGF-D, the major lymphangiogenic ligands for the receptor VEGFR-3, induce proliferation of lymphatic endothelial cells and sprouting of lymphatic vessels (10, 11). VEGFR-3-mediated lymphangiogenesis also potentially influences lymph node metastasis in various

tumor models (12-14). Recent studies by our group and others have also provided evidence for the direct contribution of VEGF to lymphangiogenesis, in addition to its principal functions in angiogenesis (15-17). Overall, targeting of the VEGFR-2 and VEGFR-3 signaling pathways are promising therapies for the treatment of solid cancers.

In prostate cancer, the expression of VEGF-C and VEGFR-3 has been shown to be highly associated with regional lymph node metastasis (18-21). Our previous studies have correlated the levels of tumor-derived VEGF-C with the extent of tumor lymphatics and subsequent lymph node and lung metastases in xenograft models of human prostate cancer (22). The precise contributions of intratumoral and peritumoral lymphatics to lymph node metastasis have been extensively debated and require further investigation (23). Recent reports have highlighted that lymphogenous spread can augment systemic metastasis (22, 24). Though angiogenesis and lymphangiogenesis are critical mediators of the metastatic process, the distinct contributions of each axis to nodal and systemic metastasis of prostate cancer remain unclear.

In the current study, we employed VEGF or VEGF-C pathway-specific therapy to decipher their roles in lymph node and lung metastasis of prostate cancer. Using over-expression and short-hairpin RNA (shRNA) silencing of these growth factors, we show that VEGF-C, and to a lesser extent VEGF, is required for lymph node and subsequent lung metastasis. Further, the findings from employing specific inhibitors of the VEGFR-2 and VEGFR-3 axes indicate that in prostate cancer, angiogenesis plays a critical role in prostate tumor growth and systemic metastasis, but targeting the VEGFR-2 axis alone does not significantly reduce tumor lymphangiogenesis or nodal metastasis. However, targeting the lymphangiogenic axis significantly reduces both lymph node and systemic

metastasis in our model, without significantly influencing primary tumor growth. Consequently, we believe that combination treatments targeting both vascular axes in conjunction with conventional therapy may offer the best protection against recurrent, disseminated disease in prostate cancer patients with a poor prognosis.

Materials and Methods

Tumor cells. The androgen-independent, androgen responsive CWR22Rv-1 tumor cell line (kind gifts from Dr. David Agus, Cedars-Sinai Medical Center, Los Angeles, CA) was maintained *in vitro* in RPMI containing 10% FBS and 1% Penicillin/Streptomycin. The androgen-dependent human prostate cancer cell line LAPC-9, was a kind gift from Dr. Charles Sawyers (Memorial Sloan Kettering Cancer Center, New York, NY). LAPC-9 xenografts were maintained *in vivo* and manipulated *ex vivo* as previously described (22).

Lentiviral production and tumor cell transduction. For all *in vivo* studies, cells were transduced using lentivirus carrying CMV promoter-driven renilla luciferase (RL) reporter genes as previously described (22). For over-expression studies, tumor cells were transduced with lentiviral vector pCCL-CMV-VEGF-C-IRES-EGFP (VEGF-C), pCCL-CMV-VEGF-C_{C156S}-IRES-EGFP (VEGF-C_{C156S}), pCCL-CMV-VEGF-IRES-EGFP (VEGF), pCCL-CMV-sVEGFR3-IRES-EGFP (sVEGFR-3), or empty vector control pCCL-CMV-IRES-EGFP (Ctrl). For short-hairpin RNA (shRNA) studies, CWR22Rv-1 cells were transduced with pRRL-U6polIII-VEGF-A-shRNA-PGKp-EGFP (shVEGF-A) or an identical vector replacing VEGF-A shRNA with irrelevant shRNA against firefly luciferase. Tumor cells were infected using viral supernatant at MOI 1 during 6 hrs incubation. Cellular expression of renilla and firefly luciferase was confirmed using an *in vitro* bioluminescence assay (Promega, Madison, WI).

Short-hairpin RNA (shRNA) interference constructs. Short hairpin constructs were generated and tested as described previously (25) using the VEGF-A target sequence, CATCACCATGCAGATTATG. Prior to generating lentiviral vectors, pRRL-vectors

were tested by transient transfection in 24-well cell culture dishes. Briefly, DNA vectors were transfected into CWR22Rv-1 cells using LipofectamineTM 2000 reagent according to manufacturer's instructions (Invitrogen, Carlsbad, CA). Specific silencing capabilities were determined at the transcription and translation levels. Candidate shRNAs were subcloned under the U6polIII promoter in pRRL-U6polIII-PGKp-EGFP.

Real-time RT-PCR analysis. Total cellular RNA was extracted from cell lines using Tri Reagent (Sigma-Aldrich, Saint Louis, MO). RNA was isolated according to the TRIzol^R procedure. RNA was quantified and assessed for purity by UV spectrophotometry and gel electrophoresis. RNA (1 µg) was reverse-transcribed using the TaqMan Reverse Transcription Reagent Kit (Applied Biosystems, Foster City, CA) according to manufacturer's instructions. The real-time PCR method and primer sequences were previously described (22).

Western blot and ELISA assays. Cell lysates were prepared from cells infected with lentiviral vectors described above using ice-cold RIPA lysis buffer containing protease inhibitor cocktail (Sigma-Aldrich, Saint Louis, MO). Protein lysates (50 µg) were separated by SDS-PAGE and transferred to a PVDF membrane. Membranes were probed using antibodies specific for human VEGFR-3 (R&D Systems, Minneapolis, MN), human VEGF-A (R&D Systems, Minneapolis, MN), or β-Actin (Sigma-Aldrich, Saint Louis, MO), followed by horseradish peroxidase-conjugated anti-IgG and detected using an enhanced chemiluminescence kit (Amersham, Pittsburgh, PA). For ELISA, cells were serum-starved with RPMI media containing 0.1% FBS overnight. Cell supernatants were collected following a 24-hour incubation. Human VEGF-A and VEGF-C concentrations were determined using the respective Quantikine ELISA assay

(R&D Systems, Minneapolis, MN) according to manufacturer's instructions. Prior to implanting cells, LAPC-9 supernatants were collected and analyzed by ELISA and western blot to ensure equivalent expression levels.

Noninvasive and *ex vivo* imaging. CWR22Rv-1 cells (5×10^5) were implanted subcutaneously above the right shoulder of immunodeficient SCID/nk^{-/-} (SCID/beige) male mice. Tumor size was measured regularly using digital calipers and by noninvasive optical imaging as follows. After administration of renilla luciferase substrate coelenterazine (1 mg/kg intravenously), anaesthetized mice (i.p. injection of a 4:1 mixture of ketamine and xylazine) were imaged as previously described (22). Primary tumors were grown to the ethical limit of 1.5 cm in diameter, at which time the animals were sacrificed.

For orthotopic implants, transduced CWR22Rv-1 cells (1×10^5 cells) or LAPC-9 cells (2.5×10^5 cells) suspended in matrigel were implanted in the surgically exposed prostate region of SCID/beige male mice as previously described (26). Cells (in 10 μ l/lobe) were implanted at the base of the exposed seminal vesicles in each dorsolateral lobe. Incisions were closed with vicryl sutures (Novartis, Somerville, NJ) and tumor growth was monitored optically over the course of the next three weeks.

MicroCT Contrast Imaging. Tumor-bearing mice were anesthetized and FenestaTM vascular contrast (VC) (Alerion, San Diego, CA) agent was injected i.v. into the tail vein and imaged after one hour. One representative animal from the control and experimental group was used for vascular contrast CT-imaging. Mice were imaged with a micro-CT scanner (MicroCAT II, Siemens Preclinical Solutions, Malvern, PA) over 7 min using 70

kVp, 500 ms exposures and 360° rotation to create images with 200-micron voxel size. CT datasets were analyzed using AMIDE software (27).

Therapeutic antibodies. Monoclonal antibodies raised against mouse VEGFR-2 (DC101) and mouse VEGFR-3 (mF4-31C1) were generated by ImClone Systems, New York (28, 29). CWR22Rv-1 cells were implanted orthotopically as described above, and mice were randomly assigned to each of the treatment groups. Therapeutic antibodies were administered i.p. at 800 ug/mouse every other day beginning three days following tumor implantation. Treatments continued until mice were sacrificed at tumor threshold.

Immunohistochemistry. Tumors, lymph nodes, and lungs were harvested and fixed in 3% paraformaldehyde overnight. Sections (5 µm) were stained with anti-Lyve-1 (RELIA Tech, San Pablo, CA) or anti-CD31 (BD Biosciences, San Jose, CA) antibodies as previously described (22). Images were processed and quantified as previously described (30). Lymphatic vessels extending into the tumor margin were classified as intratumoral lymphatics while those lacking contact with tumor cells were considered peritumoral. For orthotopic implants, Lyve-1+ lymphatics in the prostate region outside of the tumor margin were utilized in the quantification of Lyve-1+ vessel density.

Results

Induction of angiogenesis and lymphangiogenesis in the subcutaneous LAPC-9 prostate tumor model. In our experience, the androgen dependent PSA+ and AR+ LAPC-9 (31) human prostate tumor is an excellent model to study the influence of vascular growth factors on metastasis. Subcutaneously implanted LAPC-9 tumors displayed inherently low metastatic potential with few intratumoral and peritumoral lymphatics (22). However, induced expression of VEGF-C in this tumor model, to a level greater than 2-fold higher than PC-3 prostate xenografts, resulted in dramatic enhancement of intratumoral lymphangiogenesis and subsequent lymphatic metastasis (22). To further distinguish the relative roles of the lymphatic and blood vasculature in metastasis, we compared, in parallel, the effects of over-expressing VEGF, VEGF-C_{C156S} or VEGF-C in LAPC-9 tumors. The VEGF-C_{C156S} gene is a lymphatic-specific variant that lacks the angiogenic VEGFR-2 stimulatory activity of VEGF-C (32).

The tumoral blood and lymphatic vascular densities were assessed by anti-CD31 or anti-Lyve-1 staining, respectively (Fig. 1A). Over-expression of VEGF and VEGF-C enhanced blood vessel density by 2- or 3-fold over control tumors, respectively, while no significant change was observed in the VEGF-C_{C156S} over-expressing tumors. Although elevated lymphangiogenesis can be appreciated in all three groups, the localization of the Lyve-1+ vessels was distinct. The VEGF-C over-expressing tumors displayed the most dramatic increase (20-fold) in intratumoral lymphatic density, extending to depths of 1 mm within the tumor parenchyma in some regions, without an apparent increase in peritumoral lymphatics. In the VEGF-C_{C156S} over-expressing tumors, a 6-fold increase in intratumoral lymphatics was observed; however, the majority of lymphatics in the VEGF-

C_{C156S} group remained in the tumor margin. These lymphatics were surrounded by tumor cells but failed to form vascular networks at depths greater than 100 μ m. These results demonstrate the important differences in the vascular architecture induced by VEGF and VEGF-C in prostate cancer.

In accordance with differences in tumoral angiogenesis, the vascular growth factors exerted differential effects on LAPC-9 tumor growth (Fig. 1B). The VEGF tumors exhibited faster growth as they reached ethical size limit (1.5 cm in diameter) within 15 days, which is significantly faster than the control tumors at 25 days. There was no significant enhancement in the growth rate of the VEGF-C or VEGF-C_{C156S} over-expressing tumors. These data show that in our prostate cancer model, VEGF/VEGFR-2 signaling contributes to tumor growth kinetics, while VEGF-C/VEGFR-2 and VEGF-C/VEGFR-3 signaling axes do not.

Next, we measured the magnitude of metastasis in each group by *ex vivo* optical imaging. Metastases were quantified when the primary tumor reached 1.5 cm in diameter, the ethical limit. The renilla luciferase (RL) bioluminescent signal of the transduced tumor cells enabled us to quantify and compare the volume of metastasis in the ipsilateral axillary lymph nodes *in vitro* or in the dissected lung lobes in each animal (Fig. 1C). Lymph nodes from the control group displayed bioluminescent signal at ~15-fold above background luminescence. By comparison, the VEGF-C_{C156S} and VEGF-C over-expressing groups revealed dramatically higher ipsilateral axillary lymph node signals, averaging 300-fold in 6/8 mice and 1750-fold above background in 5/8 mice, respectively (Fig. 1D). Three of 8 mice in the VEGF over-expressing group also displayed elevated signal in the ipsilateral lymph node, but the intensity was

approximately 4- and 10-fold lower than that of VEGF-C and VEGF-C_{C156S}, respectively. Interestingly, VEGF-C_{C156S} and VEGF-C induced lung metastasis to similar levels (approximately 50-fold above background), which was higher than that of VEGF (18-fold). Moreover, significant metastatic lung signals were observed only in animals with lymph node metastasis, suggesting that lymph node metastasis facilitates systemic spread. It is unclear why VEGF-C_{C156S} had reduced lymphangiogenic effect, although the resulting difference highlights the importance of invasive lymphangiogenesis in metastasis, quantitatively and/or temporally. Collectively, these results suggest that lymphangiogenesis, and not angiogenesis, plays a dominant role in lymph node metastasis.

VEGF-C contributes to lymph node and systemic metastasis of the subcutaneous CWR22Rv-1 prostate tumor model. In our prior survey of several human prostate xenograft models, the androgen-independent, PSA+ and AR+ CWR22Rv-1 model displayed aggressive and metastatic growth *in vivo* (22, 33). Hence, we next investigated the influence of enhancing and suppressing lymphangiogenesis in this more aggressive model. CWR22Rv-1 cells expressing renilla luciferase (CWR/RL) were transduced with either lentivirus encoding VEGF-C, sVEGFR-3, or empty vector control. Elevated VEGF-C levels were confirmed by real-time RT-PCR (Supplementary Fig. S1A) and ELISA (Supplementary Fig. S1B) from cultured cells. No changes in VEGF-D expression were observed in response to VEGF-C over-expression (Supplementary Fig. S1A). CWR22Rv-1 tumor growth rate was not significantly enhanced in response to over-expression of VEGF-C compared to control (Fig. 2A). A significant delay in the growth rate was observed in the sVEGFR-3 over-expressing group, although tumor

growth appeared to rebound exponentially after day 16. Control tumors displayed moderate lymphatic density, with peritumoral Lyve-1+ vessels extending into the tumor margin (Fig. 2B). Scattered intratumoral lymphatic vessels, closely associated with some blood vessels, were also observed in the control tumors. VEGF-C over-expression resulted in a dramatic influx of lymphatic vessels intratumorally with reduced peritumoral lymphatic density. Intratumoral vessels were more numerous and convoluted. Conversely, sVEGFR-3 expression reduced both peritumoral and intratumoral lymphatics. Angiogenesis was slightly elevated by VEGF-C over-expression and suppressed by sVEGFR-3, although these trends were not statistically significant. The slight inhibition on tumor blood vasculature by sVEGFR-3 could likely be responsible for the delay in tumor growth *in vivo*, as there were no differences in the growth rate of each group in cell culture (data not shown).

The magnitude of CWR/RL metastasis to brachial (br) and axillary (ax) lymph nodes and lungs was measured by *ex vivo* bioluminescence signals (Fig. 2C). Compared to the control group, over-expression of VEGF-C resulted in an increase in disseminated tumor cells to regional lymph nodes and lung. In particular, VEGF-C over-expression enhanced dissemination to brachial and axillary nodes by 1.8- and 2.8-fold, respectively. Spread of tumor cells to the lung was also enhanced with VEGF-C over-expression by 1.9-fold. Conversely, the blockade of VEGF-C signal with sVEGFR-3 resulted in a significant reduction in dissemination to regional lymph nodes and lung to less than 20% and 50% of control, respectively. These results demonstrate the significant contribution of the VEGF-C/VEGFR-3 axis to regional lymph node and lung metastasis in the more aggressive androgen-independent CWR22Rv-1 prostate cancer model.

Inhibition of VEGF signaling suppresses primary tumor growth and lung metastasis. Next, we sought to investigate the relative influence of the VEGF/VEGFR-2 axis in the more aggressive CWR22Rv-1 prostate model. To this end, we generated lentivirus expressing shRNA against VEGF (shVEGF-A) under the U6 pol III promoter (25). Lentivirus expressing shRNA against the irrelevant firefly luciferase gene was used as a control (Ctrl). When CWR/RL cells were transduced with the respective shRNA lentiviral vectors at a multiplicity of infection (MOI) of 1, VEGF mRNA and secreted protein was reduced by 75% and 66%, respectively, as measured by real-time RT-PCR, ELISA, and western blot (Supplementary Fig. S1C, D). There was no significant influence on VEGF-C expression in shVEGF-A-expressing cells compared to control.

The primary tumor growth rate of shVEGF-A-expressing cells was significantly reduced compared to control (Fig. 3A). Staining of tumor sections revealed a 50% reduction in CD31+ blood vessel density in shVEGF-A-expressing tumors (Fig. 3B). There was no difference in lymphatic vasculature between Ctrl and shVEGF-A (data not shown). The reduction in angiogenesis was also observed by comparing the relative uptake of the vascular contrast agent Fenestra by microCT analysis (Fig. 3C). Note that while the Fenestra contrast uptake was normalized to the levels in the heart in both animals, the signal was significantly reduced throughout the shVEGF-A-expressing tumor.

We next asked whether a reduction in angiogenesis with shVEGF-A would reduce metastasis. VEGF knockdown had little influence on lymph node metastasis compared to control, although there was greater than 50% reduction in tumor signal in the lung (Fig. 3D). This decreased signal in the lung likely represents the direct

contribution of the tumor blood vasculature to systemic dissemination, although reduced angiogenesis and growth potential at the distal metastatic site is also a possible explanation. Importantly, metastasis was quantified when each tumor volume reached the ethical threshold, ruling out the possibility that primary tumor growth rate influenced metastatic behavior. Collectively, these data demonstrate an important role for VEGF in tumor growth and systemic metastasis, with minimal contributions to lymphangiogenesis and nodal metastasis in our model.

Blocking tumor lymphangiogenesis in orthotopic LAPC-9 tumors reduces lymph node metastasis. The stromal environment of the tumor can readily influence its metastatic behavior (34). For instance, subcutaneous LAPC-9 xenografts, in the absence of lymphangiogenic stimulus, exhibited low metastatic potential (Fig. 1) (22). Conversely, when LAPC-9 tumors are implanted in the blood and lymphatic vasculature rich environment of the mouse prostate gland, we detected a propensity for nodal metastasis even in the absence of added lymphangiogenic drive (Fig. 4, *ref.* 44). Therefore, we assessed the impact of suppressing lymphangiogenesis on tumor dissemination from orthotopically implanted LAPC-9/RL tumors. LAPC-9 tumor cells were transduced with lentiviral vectors containing either empty vector or sVEGFR-3. Repetitive optical imaging revealed comparable tumor growth rates between the control and sVEGFR-3 group (Fig. 4A). Nodal involvement in the periaortic and mesenteric lymph nodes was again assessed by using *ex vivo* bioluminescence imaging to detect the presence of tumor cells in the harvested lymph nodes. (Fig. 4B). Compared to control, metastasis to periaortic and mesenteric lymph nodes was reduced by 7- and 12-fold by sVEGFR-3, respectively. Histological analysis of lymph node sections from the control

group confirmed the presence of extensive tumor infiltration (Fig. 4C). The sVEGFR-3 group had minimal lymph node infiltration, although small subcapsular/parenchymal lesions were observed in approximately half of all the lymph nodes examined. No detectable lung metastasis was observed in either group in this study.

To examine the impact of sVEGFR-3 on tumor vasculature, we scrutinized the interface between the normal prostate region and the tumor. Control LAPC-9 tumors had extensive networks of Lyve-1+ lymphatic vessels extending throughout the normal prostate ductiles. These networks clearly aggregated around the tumor margin and extended into the tumor (Fig. 4D). Higher magnification revealed lymphatic vessels at the tumor margin intimately associated with tumor cells, which appeared to envelope some tumor cells in areas (Fig. 4D, *middle panel*, *white arrows*). By contrast, the sVEGFR-3-expressing tumors displayed different morphological characteristics in their lymphatic vasculatures. In the tumor adjacent to the normal prostatic tissues, the lymphatic networks were less elaborate and discontinuous compared to the control group. In the tumor periphery, the Lyve-1+ structures were punctate and often appeared to be isolated cells, without contiguous vessel extending into the tumor margin. Depending on proteolytic processing, VEGF-C can also influence angiogenesis by directly binding to VEGFR-2 (35). Therefore we also examined the influence of sVEGFR-3 on vascular density by comparing CD31 staining. We found no significant differences in the blood vessel density between control and sVEGFR-3-expressing tumors (Fig. 4D, *bottom panel*). These data suggest that sVEGFR-3 expression effectively suppressed VEGF-C and/or VEGF-D mediated lymphangiogenesis as well as lymph node metastasis from the prostatic microenvironment.

Effects of antibody-mediated VEGFR-2 and VEGFR-3 blockade on tumor growth and metastasis in orthotopic CWR22Rv-1 tumors. We next examined the impact of blocking the function of VEGF receptors with specific antibodies raised against murine VEGFR-3 (mF4-31C1, anti-VEGFR-3) or murine VEGFR-2 (DC101, anti-VEGFR-2). Mice bearing intraprostatic tumors of CWR/RL cells were treated with either PBS (Ctrl), anti-VEGFR-3, or anti-VEGFR-2. Primary tumor growth, assessed by noninvasive optical imaging, was not significantly different for the anti-VEGFR-3 treated group as compared to the control group (Fig. 5A). Conversely, a delay of approximately 4 days in average tumor signal was observed in the establishment of tumors in the anti-VEGFR-2 treated animals. At the end point on day 21, tumors from control and anti-VEGFR-3 treated animals were similar in size and gross morphological appearance (Fig. 5B). By contrast, tumor volume of the anti-VEGFR-2 treated group was significantly reduced by approximately 70% compared to control tumors. The tumors also appeared to be pale and less vascular than the control and anti-VEGFR-3 treated tumors. The heightened bioluminescent signals registered in the anti-VEGFR-2 treated group, relative to the other two groups, may be related to the lower hemoglobin content because hemoglobin in blood is known to absorb photons emitted by luciferase (36).

We next evaluated the impact of therapeutic antibody treatment on tumor vasculature and metastasis. Tumor sections were examined for differences in intratumoral blood and lymphatic vessel density (Fig. 5C). While anti-VEGFR-2 treated tumors showed a 62% reduction in CD31 vessel density, the reduction in Lyve-1+ lymphatic vessel density in the tumor margin was not statistically different from control. On the other hand, anti-VEGFR-3 treated tumors displayed no significant differences in

CD31+ blood vessel density but a 50% reduction in Lyve-1+ lymphatics compared to control. Unexpectedly, we noted a reduction in lymphatic density in the normal prostate region, suggesting that VEGFR-3-mediated lymphangiogenesis in the surrounding normal tissue is influenced by tumor cells. Qualitatively, the lymphatic vessels in control and anti-VEGFR-2 treated tumors had significant lymphatic density at the tumor margin with vasculature extending into the tumor. Anti-VEGFR-3 treated tumors had a general lack of lymphatic vessels at the tumor margin, with isolated Lyve-1+ cells in the normal tissue. This phenomenon was similar to what we observed with sVEGFR-3.

The impact of therapeutic antibody treatment on nodal and systemic metastasis was analyzed by *ex vivo* optical imaging (Fig. 5D). Periaortic lymph nodes and lungs isolated from control animals exhibited extensive infiltration. Blocking VEGFR-2 signaling did not significantly diminish lymph node metastasis, but resulted in a 6-fold reduction in signal in the lung. The most significant reduction in metastasis was observed in animals treated with anti-VEGFR-3 antibody, demonstrating a 4- and 5-fold reduction in periaortic lymph node and lung metastasis, respectively. Overall, these data reinforce the critical role of lymphatics in the prostate tumor margin in metastasis. These data also reflect the significance of regional dissemination to lymph nodes in the potentiation of systemic metastasis. Additionally, these data highlight the importance of VEGFR-2 inhibition in controlling systemic metastasis, without affecting lymph node metastasis.

Discussion

The notion that VEGF-C-induced lymphangiogenesis plays an important role in promoting regional lymph node metastasis is well supported in experimental models of breast cancer as well as other solid cancers (37-39). Fewer studies have explored this issue in prostate cancer, although surveys of human tissue samples have linked activation of the VEGF-C/VEGFR-3 axis with poor clinical outcome. To study the process of prostate cancer dissemination *in vivo*, we developed human prostate cancer xenograft models (22) marked with bioluminescent luciferase reporter genes to facilitate tracking of metastases. In the poorly metastatic subcutaneous LAPC-9 xenograft model, tumoral lymphangiogenesis induced by VEGF-C and VEGF-C_{C156S}, a VEGFR-3 lymphangiogenic-selective mutant, directly promoted regional nodal metastasis, which was not observed in the tumors that received the dominant angiogenic drive of VEGF (Fig. 1). Moreover, the dramatic elevation of lymphatic dissemination promoted systemic dissemination to lungs. Thus, we utilized therapeutic strategies to parse the angiogenic and lymphangiogenic contributions to nodal and systemic dissemination. In the more aggressive subcutaneous CWR22Rv-1 model, suppression of the lymphangiogenic axis with the VEGF-C ligand trap resulted in clear diminution of tumoral lymphatics, lymph node and lung metastasis (Fig. 2). On the other hand, shutdown of VEGF by shRNA diminished tumor growth and blood vasculature without a concomitant decline in nodal metastasis (Fig. 3).

In orthotopic prostate tumor models, blockade of the lymphangiogenic axis by either VEGF-C ligand trap or VEGFR-3 blocking antibody resulted in a significant decrease in lymph node metastasis but not in the growth of the prostatic tumor (Fig. 4, 5).

Conversely, abrogation of VEGFR-2 signaling with the anti-VEGFR-2 antibody significantly reduced tumor growth and blood vasculature without a corresponding reduction in nodal metastasis (Fig. 5). Collectively these findings highlight the importance of controlling tumor lymphangiogenesis, not only to prevent regional lymph node spread but also in the suppression of systemic metastasis.

One of the findings of this study highlights the fact that the site of tumor implantation can have a significant influence on the metastatic behavior of prostate tumor xenografts. Clearly, unmodified LAPC-9 tumors lack the ability to disseminate when grafted in the subcutaneous site. The low metastatic potential of LAPC-9 tumors is due in part to its very low expression of VEGF-C, relative to the moderate and high levels expressed by CWR22Rv-1 and PC-3 tumor cells, respectively (22). In contrast, orthotopic LAPC-9 tumors readily metastasize to lymph nodes, without added vascular stimulus. In the stroma of the murine prostate gland, there are ample preexisting blood and lymphatic vessels, as well as inflammatory cells, which can provide additional growth factors that stimulate vasculature. The heightened angiogenic and lymphangiogenic potential in the prostatic microenvironment, compared to the subcutaneous site could reflect reduced VEGF-C threshold levels required to promote lymphangiogenesis and nodal metastasis in prostate cancer.

The overall results presented here point to tumor lymphangiogenesis playing a more dominant role than angiogenesis in promoting lymph node and systemic metastasis in the LAPC-9 and CWR22Rv-1 prostate cancer models. An interesting corollary finding from this study is a direct connection between nodal and systemic metastasis. Previously, a report by Lin *et al.* showed that an adeno-associated virus expressing the sVEGFR-3

gene could inhibit lymph node and lung metastasis in a subcutaneous PC-3 prostate cancer model (40). Although this result points to the correlation between lymph node and lung metastasis, the low incidence of lung metastasis in the control arm of this previous study (less than 10%), precludes a firm conclusion on this issue. Three specific results reported here lend further support to the connection between lymph node and systemic metastasis. First, the lymphatic-specific VEGF-C_{C156S} promoted lymph node and lung metastasis without stimulating angiogenesis. Secondly, the development of lung metastasis was dependent on lymph node metastasis, meaning that no lung metastasis was observed in animals without nodal metastasis. Thirdly, the magnitude of lung and nodal metastasis directly correlated with each other in the four experimental groups, and the magnitude of lung signal was always lower than that in the lymph node. The latter two points suggest a sequential path of dissemination from lymph nodes to systemic sites.

The current antibody-based therapy showed that targeting VEGFR-3 signaling resulted in a dramatic reduction in nodal and systemic metastasis while blocking VEGFR-2 dominantly diminished primary tumor growth. These results corroborate with the main findings of a recent report comparing VEGFR-2 and VEGFR-3 antibody therapies in an orthotopic breast cancer model (24). However, in that study the authors observed a significant reduction in lymphangiogenesis with anti-VEGFR-2 treatment alone, which was not observed in our study. These opposing findings may reflect differences in the tumor models employed. The MDA-MB-435 breast xenograft model used in the Roberts *et al.* study required VEGF-C over-expression to gain substantial metastases. In our case, we grafted the native CWR22Rv-1 tumor cells in the murine

prostate gland. A recent study by Laakkonen *et al.* reported that VEGFR-3 blocking antibody therapy resulted in significant reduction in tumor vascular density and growth in a subcutaneous PC-3 prostate model (41). Different model systems may also be the reason that we observed a slight reduction in tumor angiogenesis without effecting tumor growth in the orthotopic CWR22Rv-1 model. Of interest, targeting the angiogenic VEGFR-2 axis did result in a significant suppression of lung metastasis but not nodal metastasis. This finding implicates the contribution of tumor angiogenesis to lung metastasis. However, we need to be mindful that the suppressive effect on lung metastasis was reached in the context of a significant reduction in primary tumor growth. In contrast, the unabated nodal dissemination would suggest that the VEGFR-2 axis is not a critical component of lymphatic metastasis in our model.

A recent study by Wong *et al.* concluded that prostate tumor lymphangiogenesis is not required for lymph node metastasis (23). By genetic modulation with VEGF-C siRNA or sVEGFR-3, they effectively down-regulated the intratumoral lymphatics in an orthotopic PC-3 xenograft model. Given a lack of suppression of nodal metastasis by these manipulations, they concluded that lymphangiogenesis was unnecessary for prostate cancer lymphatic metastasis (23). However, in this study, intratumoral lymphatics were equated to tumoral lymphangiogenesis. Yet, prior studies show that tumors often have elevated interstitial fluid pressure leading to collapsed and non-functional lymphatics within the tumor (42, 43). Instead, functional lymphatics in the tumor margin were sufficient to promote lymph node metastasis (43). In fact, the marginal lymphatics in the tumor periphery were not diminished by the inhibitory treatment in the Wong *et al.* study. In the two orthotopic prostate tumor models studied

here, we observed elaborate lymphatic vasculatures within the stroma of the normal prostatic region that extended into the tumor margin (marginal lymphatics) and a general lack of patent lymphatic vessels within the tumor. The sVEGFR-3 expressing tumors and the anti-VEGFR3-treated tumors displayed a reduction in the marginal lymphatics at the prostatic and tumoral interphase. Moreover, they also appeared to take on less invasive characteristics. Instead of being elongated and interconnected as observed in the control tumors, the Lyve-1+ lymphatics in the treated tumors were isolated and less elaborate. These findings suggest that marginal lymphatics could likely be the conduit for the lymphatic route of tumor dissemination in prostate cancer.

In this study, we were able to distinguish the contributions of angiogenesis and lymphangiogenesis to tumor growth and dissemination. Treatment that can target both vascular axes in combination with current therapeutic modalities such as radiation therapy, prostatectomy, and hormone therapy would be a rational approach to develop effective therapy to manage the most aggressive types of prostate cancer. An unresolved issue in applying anti-metastatic therapies is the timing of administration. When is it too late to initiate the treatment? What is the appropriate time to stop the treatment? These critical questions can be addressed with a prostate cancer specific molecular imaging modality. We are actively developing strategies based on the clinically relevant PET imaging for this purpose. Very recently, we were able to use a prostate-restricted gene expression vector to specifically detect nodal metastasis of prostate cancer (44). We remain hopeful that integrating molecular imaging to guide targeted therapies will improve the clinical outcome of patients with metastatic prostate cancer in the near future.

Acknowledgement

This work is supported by NCI SPORE program P50 CA092131, Prostate Cancer Foundation (to L.W), and Margaret E. Early Medical Trust award (to L.W.). J.B is supported by Department of Defense, CDMRP 07-1-0064 (prostate cancer predoctoral training grant). S.P. is supported by the career developmental program of UCLA ICMIC grant (P50 CA86306 to H.R. Herschman). We are indebted for the technical support provided by Jimmy Ou and David Stout in Crump Institute of Molecular Imaging.

References

1. Jemal A, Siegel R, Ward E, et al. Cancer statistics, 2008. *CA Cancer J Clin* 2008;58:71-96.
2. Roehl KA, Han M, Ramos CG, Antenor JACatalona WJ. Cancer progression and survival rates following anatomical radical retropubic prostatectomy in 3,478 consecutive patients: long-term results. *J Urol* 2004;172:910-4.
3. Allaf ME, Palapattu GS, Trock BJ, Carter HBWalsh PC. Anatomical extent of lymph node dissection: impact on men with clinically localized prostate cancer. *J Urol* 2004;172:1840-4.
4. D'Amico AV, Whittington R, Malkowicz SB, et al. Pretreatment nomogram for prostate-specific antigen recurrence after radical prostatectomy or external-beam radiation therapy for clinically localized prostate cancer. *J Clin Oncol* 1999;17:168-72.
5. Folkman J, Merler E, Abernathy CWilliams G. Isolation of a tumor factor responsible for angiogenesis. *J Exp Med* 1971;133:275-88.
6. Ferrara N, Gerber HPLCouter J. The biology of VEGF and its receptors. *Nat Med* 2003;9:669-76.
7. Carmeliet P. Angiogenesis in health and disease. *Nat Med* 2003;9:653-60.
8. Klement G, Baruchel S, Rak J, et al. Continuous low-dose therapy with vinblastine and VEGF receptor-2 antibody induces sustained tumor regression without overt toxicity. *J Clin Invest* 2000;105:R15-24.

9. Lee CG, Heijn M, di Tomaso E, et al. Anti-Vascular endothelial growth factor treatment augments tumor radiation response under normoxic or hypoxic conditions. *Cancer Res* 2000;60:5565-70.
10. Jeltsch M, Kaipainen A, Joukov V, et al. Hyperplasia of lymphatic vessels in VEGF-C transgenic mice. *Science* 1997;276:1423-5.
11. Veikkola T, Jussila L, Makinen T, et al. Signalling via vascular endothelial growth factor receptor-3 is sufficient for lymphangiogenesis in transgenic mice. *Embo J* 2001;20:1223-31.
12. He Y, Kozaki K, Karpanen T, et al. Suppression of tumor lymphangiogenesis and lymph node metastasis by blocking vascular endothelial growth factor receptor 3 signaling. *J Natl Cancer Inst* 2002;94:819-25.
13. Mattila MM, Ruohola JK, Karpanen T, et al. VEGF-C induced lymphangiogenesis is associated with lymph node metastasis in orthotopic MCF-7 tumors. *Int J Cancer* 2002;98:946-51.
14. Mandriota SJ, Jussila L, Jeltsch M, et al. Vascular endothelial growth factor-C-mediated lymphangiogenesis promotes tumour metastasis. *Embo J* 2001;20:672-82.
15. Nagy JA, Vasile E, Feng D, et al. Vascular permeability factor/vascular endothelial growth factor induces lymphangiogenesis as well as angiogenesis. *J Exp Med* 2002;196:1497-506.
16. Bjorndahl MA, Cao R, Burton JB, et al. Vascular endothelial growth factor-a promotes peritumoral lymphangiogenesis and lymphatic metastasis. *Cancer Res* 2005;65:9261-8.

17. Hirakawa S, Kodama S, Kunstfeld R, et al. VEGF-A induces tumor and sentinel lymph node lymphangiogenesis and promotes lymphatic metastasis. *J Exp Med* 2005;201:1089-99.
18. Zeng Y, Opeskin K, Baldwin ME, et al. Expression of vascular endothelial growth factor receptor-3 by lymphatic endothelial cells is associated with lymph node metastasis in prostate cancer. *Clin Cancer Res* 2004;10:5137-44.
19. Yang J, Wu HF, Qian LX, et al. Increased expressions of vascular endothelial growth factor (VEGF), VEGF-C and VEGF receptor-3 in prostate cancer tissue are associated with tumor progression. *Asian J Androl* 2006;8:169-75.
20. Jennbacken K, Vallbo C, Wang WDamber JE. Expression of vascular endothelial growth factor C (VEGF-C) and VEGF receptor-3 in human prostate cancer is associated with regional lymph node metastasis. *Prostate* 2005;65:110-6.
21. Roma AA, Magi-Galluzzi C, Kral MA, et al. Peritumoral lymphatic invasion is associated with regional lymph node metastases in prostate adenocarcinoma. *Mod Pathol* 2006;19:392-8.
22. Brakenhielm E, Burton JB, Johnson M, et al. Modulating metastasis by a lymphangiogenic switch in prostate cancer. *Int J Cancer* 2007;121:2153-61.
23. Wong SY, Haack H, Crowley D, et al. Tumor-secreted vascular endothelial growth factor-C is necessary for prostate cancer lymphangiogenesis, but lymphangiogenesis is unnecessary for lymph node metastasis. *Cancer Res* 2005;65:9789-98.

24. Roberts N, Kloos B, Cassella M, et al. Inhibition of VEGFR-3 activation with the antagonistic antibody more potently suppresses lymph node and distant metastases than inactivation of VEGFR-2. *Cancer Res* 2006;66:2650-7.
25. An DS, Xie Y, Mao SH, et al. Efficient lentiviral vectors for short hairpin RNA delivery into human cells. *Hum Gene Ther* 2003;14:1207-12.
26. Sato M, Figueiredo ML, Burton JB, et al. Configurations of a two-tiered amplified gene expression system in adenoviral vectors designed to improve the specificity of in vivo prostate cancer imaging. *Gene Ther* 2008.
27. Loening AM, Gambhir SS. AMIDE: a free software tool for multimodality medical image analysis. *Mol Imaging* 2003;2:131-7.
28. Pytowski B, Goldman J, Persaud K, et al. Complete and specific inhibition of adult lymphatic regeneration by a novel VEGFR-3 neutralizing antibody. *J Natl Cancer Inst* 2005;97:14-21.
29. Witte L, Hicklin DJ, Zhu Z, et al. Monoclonal antibodies targeting the VEGF receptor-2 (Flk1/KDR) as an anti-angiogenic therapeutic strategy. *Cancer Metastasis Rev* 1998;17:155-61.
30. Cao R, Brakenhielm E, Pawliuk R, et al. Angiogenic synergism, vascular stability and improvement of hind-limb ischemia by a combination of PDGF-BB and FGF-2. *Nat Med* 2003;9:604-13.
31. Klein KA, Reiter RE, Redula J, et al. Progression of metastatic human prostate cancer to androgen independence in immunodeficient SCID mice. *Nat Med* 1997;3:402-8.

32. Joukov V, Kumar V, Sorsa T, et al. A recombinant mutant vascular endothelial growth factor-C that has lost vascular endothelial growth factor receptor-2 binding, activation, and vascular permeability activities. *J Biol Chem* 1998;273:6599-602.
33. Holleran JL, Miller CJ, Culp LA. Tracking micrometastasis to multiple organs with lacZ-tagged CWR22R prostate carcinoma cells. *J Histochem Cytochem* 2000;48:643-51.
34. De Wever OM, Mareel M. Role of tissue stroma in cancer cell invasion. *J Pathol* 2003;200:429-47.
35. Joukov V, Pajusola K, Kaipainen A, et al. A novel vascular endothelial growth factor, VEGF-C, is a ligand for the Flt4 (VEGFR-3) and KDR (VEGFR-2) receptor tyrosine kinases. *Embo J* 1996;15:1751.
36. Zhao H, Doyle TC, Coquoz O, et al. Emission spectra of bioluminescent reporters and interaction with mammalian tissue determine the sensitivity of detection in vivo. *J Biomed Opt* 2005;10:41210.
37. Skobe M, Hawighorst T, Jackson DG, et al. Induction of tumor lymphangiogenesis by VEGF-C promotes breast cancer metastasis. *Nat Med* 2001;7:192-8.
38. Karpanen T, Egeblad M, Karkkainen MJ, et al. Vascular endothelial growth factor C promotes tumor lymphangiogenesis and intralymphatic tumor growth. *Cancer Res* 2001;61:1786-90.
39. Alitalo K, Carmeliet P. Molecular mechanisms of lymphangiogenesis in health and disease. *Cancer Cell* 2002;1:219-27.

40. Lin J, Lalani AS, Harding TC, et al. Inhibition of lymphogenous metastasis using adeno-associated virus-mediated gene transfer of a soluble VEGFR-3 decoy receptor. *Cancer Res* 2005;65:6901-9.
41. Laakkonen P, Waltari M, Holopainen T, et al. Vascular endothelial growth factor receptor 3 is involved in tumor angiogenesis and growth. *Cancer Res* 2007;67:593-9.
42. Jain RK. Barriers to drug delivery in solid tumors. *Sci Am* 1994;271:58-65.
43. Padera TP, Kadambi A, di Tomaso E, et al. Lymphatic metastasis in the absence of functional intratumor lymphatics. *Science* 2002;296:1883-6.
44. Burton JB, Johnson, M., Sato, M., Koh, S.S., Mulholland, D., Stout, D., Chatziioannou, A.F., Phelps, M, Wu, H., Wu, L. . Adenovirus Mediated Gene Expression Imaging to Directly Detect Sentinel Lymph Node Metastasis of Prostate Cancer. *Nature Medicine* 2008;In Press.

Figure Legends

Figure 1. Induction of angiogenesis and lymphangiogenesis in the subcutaneous LAPC-9 prostate tumor model. SCID/beige mice were implanted with LAPC-9 tumor cells expressing renilla luciferase and the respective growth factor (VEGF-A, VEGF-C, VEGF-C_{C156S} or empty vector control). *A*, Tumors were fixed, sectioned and stained with antibodies recognizing blood vessels (CD31) and lymphatic vessels (Lyve-1). Blood vessels were distributed throughout the tumor section while lymphatics were predominantly in the tumor margin (tumor edge is marked by white dotted line). Vessel quantification was performed from at least 5 representative areas from each tumor for CD31+ blood vessels (*A*, *CD31*) and Lyve-1+ lymphatic vessels (*A*, *Lyve-1*). Overall counts were normalized by area and represented as a percentage compared to control. *B*, Tumor growth was monitored by caliper measurements every four days once tumors became palpable (length x width x 0.52). When tumors reached ethical size limit, animals were sacrificed and skin was peeled back to expose regional axillary lymph nodes. *C*, Representative images of animals from each group revealed photon emission in the ipsilateral but not in contralateral axilla. Lungs were dissected into separate lobes and imaged. *D*, Bioluminescent signals from ipsilateral lymph node (LN) or lung of all animals in a cohort were averaged and normalized to background luminescence. The number of animals in each cohort that displayed significant metastasis by bioluminescent signals is listed above each bar. Optical scale bars are in photons/second/cm²/steradian (p/s/cm²/sr) and histology bar represents 20 μ m. (*p < 0.05; **p < 0.01; n = 6-8)

Figure 2. Intratumoral lymphangiogenesis in subcutaneous implants of CWR22Rv-1 is modulated by VEGF-C signaling. A, CWR22Rv-1 tumor cells expressing VEGF-C or sVEGFR-3 or empty vector (Ctrl) were implanted in SCID/beige mice and tumor volume was monitored by caliper measurements until tumors reached ethical size limit. B, Representative tumor sections displaying the tumor margin (white dotted line) delineating the intratumoral and peritumoral lymphatics (*Lyve-1*, red) and blood vessels (*CD31*, green) in CWR22Rv-1 tumors expressing the respective proteins. Lower panel are representative sections displaying the intratumoral Lyve-1+ and CD31+ vasculature. Intratumoral (left of dotted line) Lyve-1+ and CD31+ areas were quantified for all tumors in each group (n = 4) and presented as percent control. No significant differences in CD31 vessel density were detected. C, *Ex vivo* optical signal was detected in indicated organs from representative animals (*Ax*, axillary; *Br*, brachial; lung). Bioluminescent signal intensity from each tissue was averaged for all animals in each group (C; *graphs, Lymph Node and Lung*). *p < 0.05; **p < 0.01.

Figure 3. VEGF-A shRNA reduces tumor growth, blood vessel density, and systemic metastasis, without effecting lymph node metastasis. CWR22Rv-1 cells (5 x 10⁵) transduced with lentivirus expressing short-hairpin RNA directed against firefly luciferase (*Ctrl*) or VEGF-A (*shVEGF-A*) were implanted subcutaneously on the shoulder of SCID/beige mice and tumor volume was monitored, A. Delay in tumor growth was observed in the shVEGF-A group. B, Histological analysis of tumor sections revealed 50% reduction in CD31+ tumor vasculature. C, microCT analysis using FenestraTM vascular contrast agent in representative animals revealed a reduction in contrast agent

accumulation in the tumor despite similar accumulation within the heart. *D*, Following sacrifice and dissection, *ex vivo* optical signal was detected in indicated organs from representative animals (*Ax*, axillary LN; *Br*, brachial LN; lung). Maximum bioluminescent signal intensity from each tissue was averaged for all animals in each group and represented in the respective graph (Lymph Node and Lung). Optical scale bars are in p/s/cm²/sr; error bars are \pm SEM, n = 4, **p < 0.01.

Figure 4. sVEGFR-3 reduces metastasis to regional lymph nodes in orthotopic LAPC-9 tumors. *A*, Tumor-mediated optical signal (Ctrl, LAPC-9/RL/GFP; sVEGFR-3, LAPC-9/RL/sVEGFR3/GFP) in all mice (n = 10/group) shown during exponential growth phase at day 10 and 15 following orthotopic implantation. *B*, On day 16, mice were sacrificed and periaortic and mesenteric lymph nodes were removed and imaged *ex vivo* for renilla luciferase activity. *C*, Histological analysis of H&E stained sections revealed the presence of extensive metastasis throughout the periaortic lymph nodes of mice from control group (*Ctrl*) while lymph nodes from mice bearing sVEGFR-3 over-expressing tumors showed reduced metastasis (images to the right represent higher magnifications encompassed by the boxes). *D*, LAPC-9 tumors were fixed, paraffin embedded, and sectioned through the junction of the seminal vesicles to reveal the interface of the prostate, seminal vesicle, and tumor xenograft. Lyve-1+ lymphatics (in red) around the tumor margin and extending into the tumor were more profound in the controls compared to the punctate, disorganized lymphatics surrounding tumors expressing sVEGFR-3 (*D, top panel*). Higher magnification revealed the presence of numerous marginal lymphatics (often containing tumor cells, white arrow) in the control

group (*D*, *middle panel*). No difference was observed in intratumoral angiogenesis between control and sVEGFR-3 as indicated by CD31 staining (*D*, *bottom panel*). Pros. = prostate, Optical scale bars are in p/s/cm²/sr, histology scale bar is C = 100 μ m and D = 20 μ m, *p < 0.05.

Figure 5. Orthotopic CWR22Rv-1 tumor growth characteristics with VEGFR-3 and VEGFR-2 blocking antibody treatment. CWR22Rv-1 tumors expressing renilla luciferase were orthotopically implanted in SCID/beige mice (n = 5/group). Treatment began three days post-implantation (Ctrl, PBS; α -R3, anti-VEGFR-3; α -R2, anti-VEGFR-2) with i.p. injections of 800 μ g/mouse of each antibody (100 μ l) every other day. *A*, Representative images of optical signal in mice over the course of tumor growth for up to 20 days. All groups were sacrificed at comparable signal intensity (Ctrl and α -R3 were sacrificed at day 17, α -R2 were sacrificed at day 20). Averaged optical signal intensity over the course of tumor growth (middle graph) indicated a delay in optical signal in tumors of α -R2 treated animals. Upon sacrifice, tumors and adjoined seminal vesicles were removed, photographed and measured. The α -R3 treated group displayed no significant differences in tumor volume compared to control, while α -R2 treatment reduced tumor volume and vascularity, *B*, *C*, Tumors harvested from the respective treatment group were stained for blood (CD31) and lymphatic (Lyve-1) vessels. The treatment effects on vessel densities were measured and shown in the respective graph. *D*, Periaortic lymph nodes (*PA*) and lungs from the respective treatment groups were dissected and imaged *ex vivo* for renilla luciferase signal. Averaged luminescence signals from periaortic lymph nodes and lung are shown in respective graphs. Scale bars B =

1cm and $C = 20 \mu\text{m}$, optical scale bars are in $\text{p/s/cm}^2/\text{sr}$; error bars are $\pm\text{SEM}$; $*p<0.05$, $**p<0.01$; $n = 5$.

Supplemental Figure S1

Transduction of CWR22Rv-1 cells with lentivirus expressing VEGF-C resulted in high-level expression as measured by real time RT-PCR, *A*, and ELISA, *B*. *C*, VEGF-A expression was reduced by 75% in VEGF-A shRNA-expressing cells compared to control. Control and shVEGF-A expressing cells remain unaffected in expression of VEGF-C. *D*, Supernatants from the same cells show reduced secretion of VEGF-A by ELISA.

Figure 1

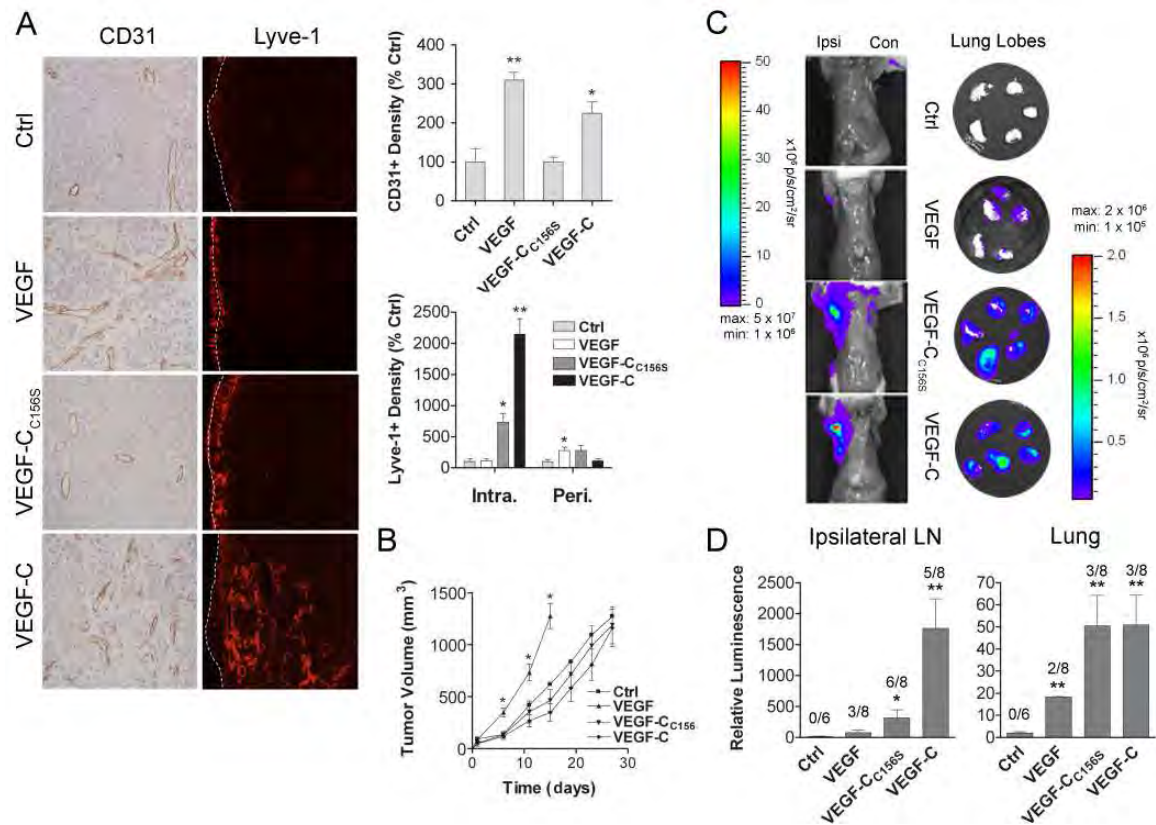


Figure 2

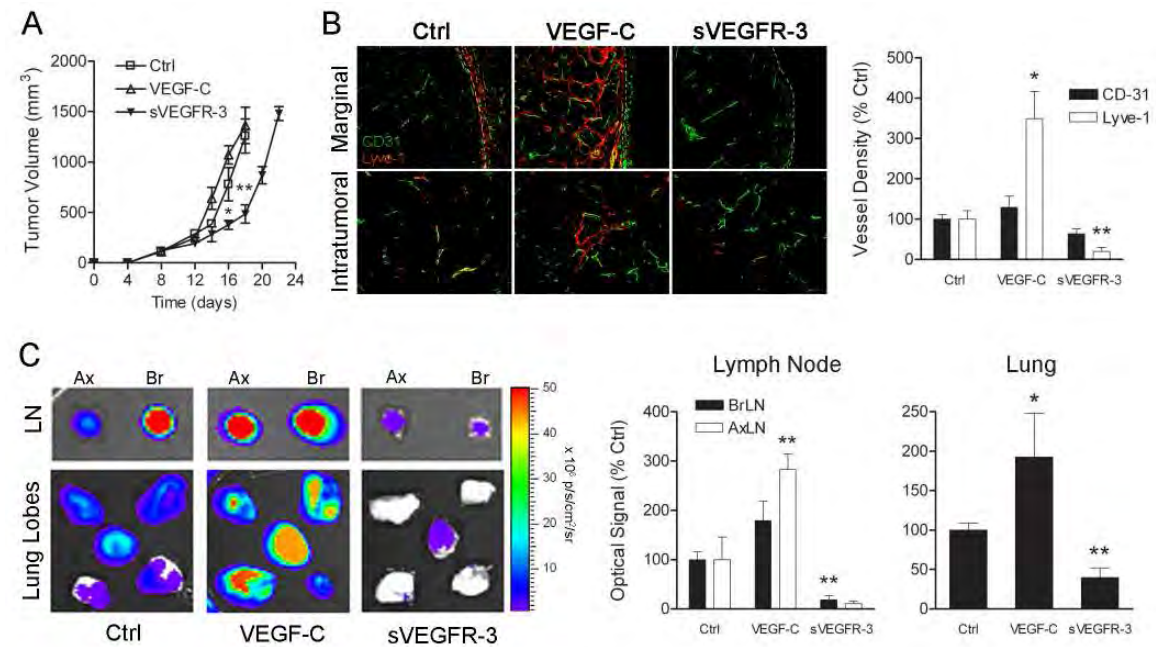


Figure 3

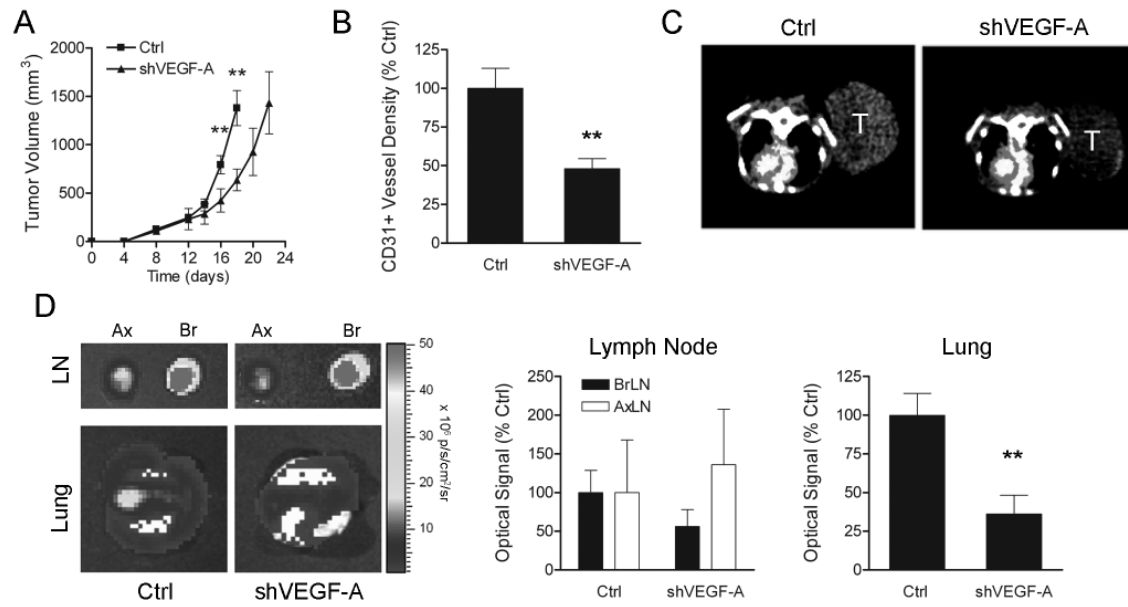


Figure 4

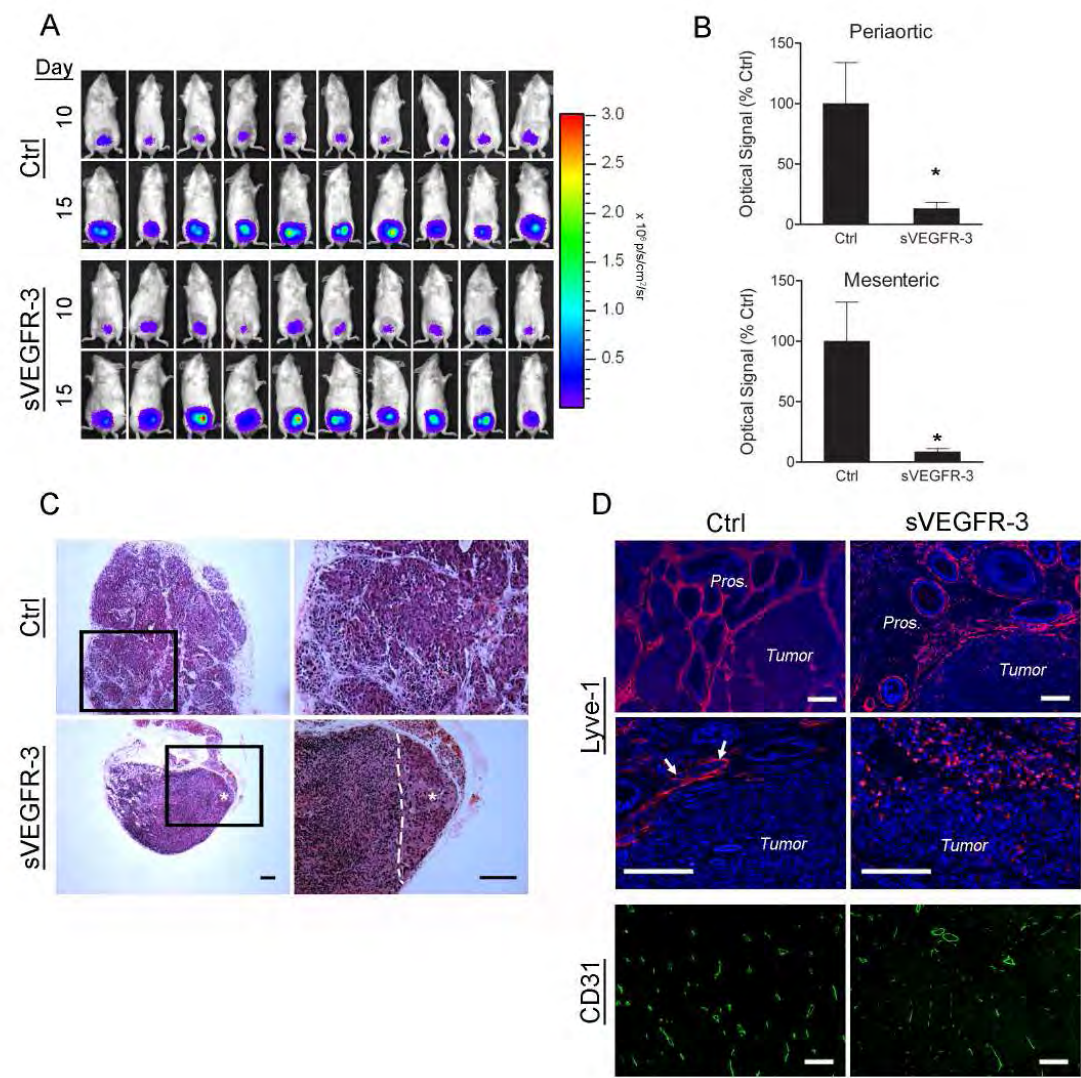
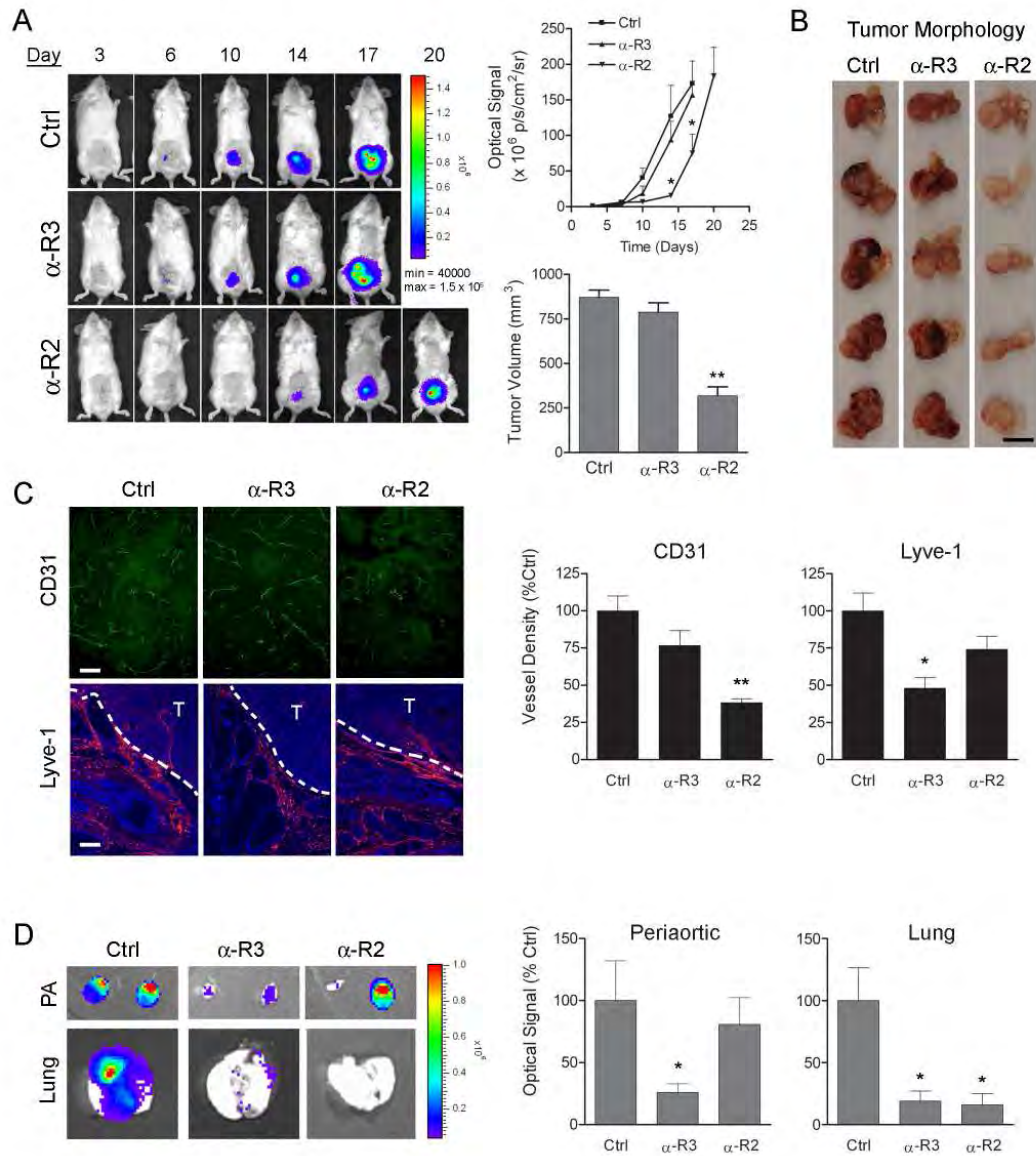
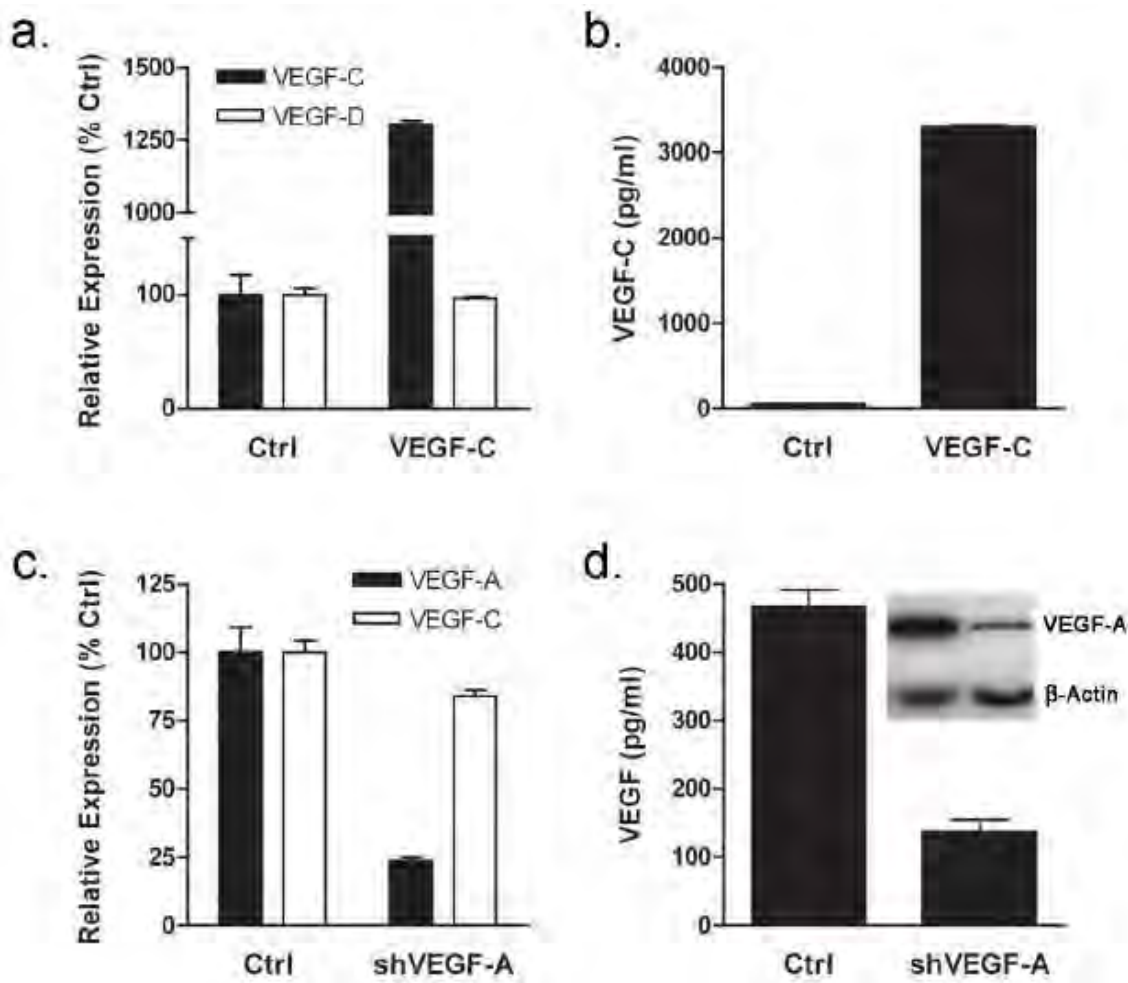


Figure 5



Supplemental Figure 1



Jeremy B. Burton

3901 Bixby Dr.
La Verne, CA 91750

Tel: (818) 288-4902
jburton@mednet.ucla.edu

Profile

Motivated, creative, and technically proficient molecular and cellular biologist with extensive experience working with cancer models to study tumor biology in mice. My major focus has been integrating practical tumor biology techniques with state of the art imaging modalities to improve and enhance the understanding of tumor angiogenesis, lymphangiogenesis, and metastasis.

- Highly independent and thoughtful researcher.
- Strong bench skills with focused attention to detail.
- Can effectively lead and manage research groups and projects.
- Diverse publications in major scientific journals.

Selected Technical Skills

Molecular/Cellular Biology: General molecular cloning procedures, PCR, Real time PCR, RNA interference, recombinant protein expression and purification, promoter/reporter assays, SDS-PAGE, immunoprecipitation, blotting, RNA Isolation/Purification, Immunohistochemistry, cell-based migration and proliferation assays.

Virology/Immunology: Lentiviral Propagation/titration, Retroviral Propagation/titration, Phage Production, Plaque Assays, Neutralization assays, ELISA.

In Vivo Techniques: All injection routes, breast and prostate orthotopic xenografting, survival surgery, lymph node sampling, primary cell suspensions, genotyping, microPET, microCT, bioluminescence and fluorescence imaging.

Education

- **Doctor of Philosophy (PhD)** Degree in Medical and Molecular Pharmacology; June 2008
University of California, Los Angeles. PI: Dr. Lily Wu
Dissertation Topic: My doctoral research has been focused on evaluating the metastatic behavior of prostate xenografts using optical and PET imaging to track tumor cells. This research focused on the impact of lymphatic vasculature on systemic metastasis and the relative role of the orthotopic environment on metastatic behavior. I applied over-expression, RNAi, and therapeutic antibody strategies to inhibit tumor blood and lymphatic vasculature and evaluate the impact on metastasis, growth, and progression of prostate cancer. My studies also focused on the targeting and detection of lymph node metastasis in mice using adenovirus-mediated gene expression imaging.
- **Masters of Science (MS)** Degree in Biology; June 2002
California State Polytechnic University Pomona, CA. PI: Dr. Bijay Pay
Thesis topic: Retroviral RNA dimerization and packaging
- **Bachelor of Science (BS)** Degree in Biotechnology; June 1999
California State Polytechnic University Pomona, CA.

Research experience

- **Graduate Student Researcher**, 2002 – Present
University of California, Los Angeles. Department of Molecular and Medical Pharmacology.
Mastered molecular techniques and animal models in the study of tumor angiogenesis/lymphangiogenesis
- **Teaching Associate**, 1999 – 2002
California Polytechnic University, Pomona, CA. Biology Department.
Taught undergraduate laboratory course in Recombinant DNA techniques, Virology, and Electron Microscopy.
- **Graduate Research Assistant**, 1999 – 2002
California Polytechnic University, Pomona, CA. Biology Dept.
Conducted an analysis of the Moloney-MLV retroviral RNA dimerization region using tethered-ribozymes, which led to Masters degree.
- **Field Technician**, 1997
Department of Fish and Wildlife, San Diego, CA.
Assisted in the collection, processing, and cataloging of reptiles for corridor surveys in Riverside County.

Honors/Awards

- *Department of Defense Predoctoral Training Grant in Prostate Cancer*, 2007 – 2009
- *Multimodality image of the year*, 2007
Society of Molecular Imaging Annual Meeting
- *Travel Award*, 2007
Academy of Molecular Imaging/Society of Molecular Imaging (AMI/SMI)
- *Young Investigator Award*, 2007
2nd International Symposium on Cancer Metastasis and the Lymphovascular System
- *NIH Research Training in Pharmacological Sciences/University Training Grant*, 2003 – 2006.
- *Molecular Pharmacology Retreat Award*, 2003
University of California, Los Angeles

Publications

- Johnson, M., Sato, M., **Burton, J.B.**, Gambir, S.S., Carey, M., and Wu, L. (2005). Micro-PET/CT Monitoring of Herpes Thymidine Kinase Suicide Gene Therapy in a Prostate Cancer Xenograft: The Advantage of a Cell-specific Transcriptional Targeting Approach. *Molecular Imaging*. 4(2), 2005, pp. 1 – 10.
- Björndahl, M.A., Cao R., **Burton, J.B.**, Brakenhielm, E., Religa, P., Galter, D., Wu, L., and Cao, Y (2005). VEGF-A promotes tumoral lymphangiogenesis and lymphatic metastasis. *Cancer Res*. October 15, 2005; 65(20): 9261 - 9268.

- Johnson, M., Huyn, S., **Burton, J.B.**, Sato, M., and Wu L. (2006). The Differential Biodistribution of Adenoviral Vector In Vivo as Monitored by Bioluminescence Imaging and Quantitative PCR. *Human Gene Therapy*. 2006 Dec. 17(12): 1262-9.
- Brakenhielm, E.*, **Burton, J.B.***, Johnson, M., Chavarria, N., Morizono, K., Chen, I., Alitalo, K., Wu, L. (2007) Modulating metastasis by a lymphangiogenic switch in prostate cancer. *Int. J. Cancer*. **121** (10) p. 2153-61.
- Sato, M., Figueiredo, M. L., **Burton, J.B.**, Johnson, M., Chen, M., Powell, R., Gambhir, S. S., Carey, M., Wu, L. (2008) Configurations of a two-tiered amplified gene expression system in adenoviral vectors designed to improve the specificity of in vivo prostate cancer imaging. *Gene Ther*. **15** (8) p. 583-93.
- **Burton, J.B.**, Johnson, M., Sato, M., Koh, S., Stout, D., Chatziioannou, A.F., Phelps, M., Wu, L. (2008). Adenovirus Mediated Gene Expression Imaging to Directly Detect Sentinel Lymph Node Metastasis of Prostate Cancer. *Nat. Med.* **14** (8) p. 882-8.
- **Burton, J.B.**, Priceman, S.J., Sung, J.L., Pytowski, B., Alitalo, K., Wu, L. (2008). Suppression of Prostate Cancer Nodal and Systemic Metastasis by Blockade of the Lymphangiogenic Axis. In Press *Cancer Res*. October 2008.

(* Co-first Author)

References

- *Professor, Lily Wu, MD, PhD.*
Dissertation Chair/PI
University of California, Los Angeles
Phone: (310) 794-4390
Email: lwu@mednet.ucla.edu
- *Professor, Luisa Iruela-Arispe, PhD.*
Dissertation Committee Member
University of California, Los Angeles
Molecular, Cellular, and Developmental Biology Dept.
Phone: (310) 794-5763
Email: arispe@mbi.ucla.edu
- *Professor, Asim Dasgupta, PhD.*
Dissertation Committee Member
University of California, Los Angeles
Microbiology, Immunology, and Molecular Genetics Dept.
Phone: (310) 206-8649
Email: dasgupta@ucla.edu